Phenotypes of *Pinus sylvestris* are more coordinated under harsher conditions across Europe

Raquel Benavides[1,2], Bárbara Carvalho[1], Silvia Matesanz[3], Cristina C. Bastias[1,4], Stephen Cavers[5], Adrián Escudero[3], Patrick Fonti[6], Elisabet Martínez-Sancho[6] and Fernando Valladares[2,3]

[1]Departamento de Biogeografía y Cambio Global. Museo Nacional de Ciencias Naturales. CSIC. C/José Gutiérrez Abascal 2, 28006, Madrid, Spain.

[2] Centro de Estudos Florestais, Instituto Superior de Agronomia, Universidade de Lisboa, Tapada da Ajuda, 1349-017 Lisboa, Portugal.

[3]Área de Biodiversidad y Conservación, Universidad Rey Juan Carlos, c/ Tulipán, s/n. 28933, Móstoles, Spain.

[4]UMR 5175 CEFE, Univ. Montpellier, CNRS, EPHE, IRD, Univ. Paul Valéry, Montpellier, France.

[5]UK Centre for Ecology & Hydrology, UK CEH Edinburgh, Bush Estate, Penicuik, Scotland. EH26 0QB.

[6]Swiss Federal Research Institute for Forest, Snow and Landscape Research WSL, Birmensdorf, Switzerland.

Correspondence: R. Benavides (rbenavidescalvo@gmail.com, +34 91 411 13 28)

ABSTRACT

1. Plant species that grow across environmental gradients show a range of trait expression, but traits do not vary independently. In fact, phenotypes are integrated expressions of multiple traits that covary due to trade-offs among functions and processes. Understanding trait covariation structures will ultimately help with predicting species' responses to change and developing management actions.
2. We measured variation and covariation (a proxy of phenotypic integration) among functional traits of *Pinus sylvestris* from paired populations across its European distribution. Populations within a pair were close enough to be in gene flow contact but located in contrasting environmental conditions across a local gradient. Measured traits represented three axes of variation (groups of traits) related to a tree's competitive ability and the trade-off between resource acquisition and conservation, namely plant size measures and stem and foliar traits.
3. Results revealed important intra- and inter-population trait variability. In particular, at the population level, trait means shifted across the climatic gradient mainly described by mean annual temperature. Moreover, we found a higher degree of trait covariation in populations under harsher environments. This pattern was consistent within population pairs, suggesting that higher trait covariation may be adaptive, being more coordinated in sites with harsher conditions. At larger spatial scales, we found a less conclusive pattern with a trend of increasing covariation at the northern edge of the species distribution. This result suggests that at larger scales different processes may be involved in the trade-off between the adaptive value of phenotypic covariation vs. its constraints on trait combinations that may limit plant's response capability.
4. Synthesis: trait covariation varies at different spatial scales, increasing under harsher conditions, and the robustness and repeatability of this pattern suggests its adaptive role for the species' responses to different environments.

Keywords: Adaptive response, functional traits, intraspecific variability, multi-scale gradients, phenotypic integration, plant-environment interaction, Scots pine, trait covariation.

RESUMEN

1. Las especies vegetales muestran diferencias en la expresión de sus rasgos a lo largo de gradientes ambientales; sin embargo, éstos no varían de manera independiente. El fenotipo es la expresión integrada de rasgos que covarían debido a los distintos procesos bajo las condiciones a los que están sometidos. Comprender la estructura de covariación entre rasgos puede ayudar a predecir la respuesta de las especies frente a los cambios y a anticipar medidas de gestión frente a los mismos.
2. En este trabajo, hemos medido la variación y covariación (aproximación a la integración fenotípica) entre rasgos funcionales en individuos de *Pinus sylvestris* procedentes de pares de poblaciones a lo largo de su área de distribución europea. Las poblaciones dentro de una pareja estaban lo suficientemente cerca para asumir flujo genético entre ellas, pero localizadas en condiciones contrastadas en un gradiente local. En cada población medimos rasgos funcionales pertenecientes a tres ejes de variación relacionados con la capacidad competitiva del individuo y de la economía de los recursos (el equilibrio entre la adquisición y conservación de recursos), en concreto medidas de tamaño de la planta y rasgos medidos en tronco y hojas.
3. Los resultados revelaron una importante variabilidad de rasgos a nivel intra- e inter-poblacional. En concreto, la media poblacional de la mayoría de los rasgos varió a lo largo del gradiente climático definido principalmente por la temperatura media anual. Además, encontramos un grado de covariación de rasgos mayor en poblaciones bajo condiciones ambientales más duras. Este patrón fue consistente entre parejas de poblaciones, sugiriendo que la covariación de rasgos puede ser adaptativa apareciendo fenotipos más coordinados en ambientes menos favorables. A escala espacial mayor, encontramos una

tendencia con mayor covariación en el extremo norte del área de distribución. Este resultado asimétrico entre los extremos de la distribución, aunque no concluyente, indica que a grandes escalas otros procesos pueden intervenir en el balance entre el valor adaptativo de la covariación y la limitación que impone en la combinación de rasgos que pueden mermar la capacidad de respuesta frente a cambios.

4. Síntesis: la covariación de rasgos varía a diferentes escalas espaciales, incrementándose en condiciones estresantes. La robustez de dicho patrón sugiere su papel adaptativo en la respuesta de las especies frente a diferentes ambientes.

Palabras clave: covariación de rasgos, gradientes multi-escala, integración fenotípica, interacción planta-ambiente, pino silvestre, rasgos funcionales, respuesta adaptativa, variabilidad intraespecífica.

INTRODUCTION

Plant functional traits are an expression of a combination of individual use of resources and adaptation to a given environment (Grime, 1977; Westoby et al., 2002; Leimu & Fischer, 2008). Thus, within a species, traits may vary geographically as a response to environmental gradients at different scales, capturing individual (e.g. Benavides, Scherer-Lorenzen et al., 2019) and population responses (e.g. Abdala-Roberts et al., 2017; Luo et al., 2019). Previous works have studied intraspecific trait variability across wide study areas with changes in altitude and latitude (Fajardo & Piper, 2011; Laforest-Lapointe et al., 2014; Umaña & Swenson, 2019), demonstrating that trait–environment relationships are excellent candidates to predict species responses to environmental changes (Albert et al., 2010; Jung et al., 2014). They also showed that, although plant species may have the potential for highly plastic responses, strong environmental gradients impose ecological limits on these responses, which are specific for each trait (Valladares et al., 2007; Umaña & Swenson, 2019). In fact, most of these patterns come from studying responses of traits in isolation, or multiple traits but from a univariate perspective (but see e.g. Laforest-Lapointe et al., 2014; Umaña & Swenson, 2019; Benavides, Valladares et al., 2019).

Phenotypes are much more than the sum of multiple traits. Their integration reflects trade-offs among functions (Pigliucci, 2003; Bonser, 2006) and life history strategies (Chave et al., 2009; Westoby, 1998; Wright et al., 2004), and their responses under different environmental conditions (Maire et al., 2013). Thus, great interest is emerging to understand how traits covary to shape a phenotype, how these relationships vary across gradients and scales, and the adaptive role of trait combinations in different environments. Phenotypic integration is not a new concept within evolutionary ecology (Olson & Miller, 1958; Berg, 1960), although it has only been addressed intermittently due to the lack of a clear conceptual framework for empirical and theoretical studies (Pigliucci, 2003). Since the 2000s, a generation of studies has developed new state-of-the-art techniques, amassed evidence and identified challenges for future research

on the topic (Pigliucci, 2003; Pigliucci, 2004; Hallgrímsson et al., 2009; Armbruster et al., 2014; Klingerber, 2014). Thereafter, phenotypic integration, strictly speaking, has been defined as the functional, genetic or developmental disposition or propensity to produce trait covariation, i.e. the correlation structure measured directly among traits (also known as statistical integration *sensu* Armbruster et al., 2014). The trait covariation structure (statistical integration) is then necessary to assess phenotypic integration, which is an intrinsic characteristic of organisms, influencing species evolvability by producing correlated responses in other traits under selection (Wagner et al., 2007; Hallgrímsson et al., 2009).

The analysis of trait covariation is currently used in other disciplines within ecology to infer underlying mechanisms of species coexistence (Kraft et al., 2015; Dwyer & Laughlin, 2017a; Benavides, Scherer-Lorenzen et al., 2019; Benavides, Valladares et al. 2019), to describe the adaptive strategies of species (Boucher et al., 2013; Messier et al., 2018; Anderegg et al., 2018; Rosas et al., 2019; Carvalho et al., 2020; Damián et al., 2020) or to describe phenotypic diversity across gradients (between and within species), i.e. specific syndromes in response to the environmental variation (Wright et al., 2004; Laforest-Lapointe et al., 2014; Dwyer & Laughlin, 2017a; Umaña & Swenson, 2019). From these studies, a couple of general patterns have arisen. First, increasing stress usually leads to strong directional selection pressures (Boucher et al., 2013) that filter out unsuitable trait combinations and favour higher trait covariance (Westoby & Wright, 2006; Dwyer & Laughlin 2017a) and functional convergence (i.e. trait similarity) among coexisting species (Boucher et al., 2013; Dwyer & Laughlin, 2017a). Second, trait covariation structures are not always conserved across scales because responses to environmental drivers across gradients are trait-specific. For instance, the well-known global leaf economic spectrum (leaf traits closely correlated along a continuum, involving a trade-off between conservation and acquisition of resources, Wright et al., 2004; Reich et al., 2014) or the trade-off between hydraulic safety and efficiency (conduits' characteristics fostering either xylem transport or protection against embolism) are not always

reproduced at fine spatial scales or within communities/populations (Gleason et al., 2015; Messier et al. 2017; Anderegg et al., 2018; Rosas et al., 2019; Carvalho et al., 2020).

Although emerging knowledge is helping to re-construct the phenotypic integration concept by including patterns of trait variation, it remains almost unknown whether trait covariation within species is maintained along gradients and scales, or whether it varies according to the specific selective pressure (see for intraspecific trait covariation across gradients at a single scale Anderegg et al., 2018 and Umaña & Swenson, 2019). Conserved patterns may reveal genetic and developmental constraints or consistent past selection towards certain trait combinations (Westoby et al., 1995). Alternatively, different trait means and covariation patterns may indicate the role of divergent selection (Ambruster et al., 2004), boosting or discarding certain trait combinations in given environments (Berg, 1960; Cheverud, 1984; Wagner et al., 2007; Damián et al., 2018) through the *plasticity of integration* (*sensu* Pigliucci, 2003), i.e. the integration's ability to vary under different conditions.

In this study, for the first time we analysed the phenotypic response of a tree species, *Pinus sylvestris*, in terms of variation and covariation of functional traits across a large part of its range and at different spatial scales. *Pinus sylvestris* is the most widely distributed pine species in the world and grows from Mediterranean mountains up to boreal forests in Fennoscandia and East Siberia, encompassing a wide range of climatic conditions (Carlisle & Brown, 1968). Given the range of environmental variation it experiences, the evaluation of changes in the phenotypic space and trait covariation for this species offers great potential for insight into the role played by trait covariation in the responses of the species. Specifically, we surveyed more than 500 trees from 20 populations across its European distribution (from Spain to Finland, and from Greece to the United Kingdom). Most populations were sampled in paired sites occupying locally contrasting conditions (such as elevation or water availability), but with significant potential for gene flow among them. This design followed Lotterhos and Whitlock (2015), which suggested that sampling populations in pairs across a species' range minimises the

neutral genetic differences between sampled populations and therefore improves the power to detect signatures of selection. In our study, this novel design combining a wide spatial scale approach (European distribution) with local environmental gradients (pairs) allowed us to explore the effect of the environment on trait covariation. Thus, we analysed the distribution of trait variability, sought the main environmental drivers of this variability, and studied trait covariation (statistical integration) at two scales, i.e. across local gradients and species range. Our aim was to understand trait responses to environmental variation at both scales, and to search for trait covariation patterns indicative of adaptive strategy in this pine species. We assumed that the environmental suitability decreases towards the edges of the species distribution and, therefore, peripheral populations face more stressful conditions with respect to the species' optimum condition in central populations (Soulé, 1973; Sexton et al. 2009). Under this assumption, we hypothesised that trees in central populations would have more acquisitive phenotypes, i.e. larger trees with more productive needles (e.g. larger with higher N content, Wright et al., 2004; 2017), while those in peripheral populations would probably exhibit a more conservative strategy (e.g. smaller, less productive but more long-lasting needles). We also expected that more coordinated phenotypes would be expressed in harsher conditions for the species (reduced environmental suitability), where populations would have experienced more severe filters, and only individuals with a given set of trait values would have survived. Moreover, we hypothesised that in the core of the distribution local environmental heterogeneity (e.g. soil characteristics, high altitudes or water availability) may impose harsher conditions on some populations in a similar way to which it occurs in peripheral populations (Soulé, 1973), driving convergence of conservative traits and more coordinated phenotypes.

MATERIAL AND METHODS

Study design and sites

189 Twenty populations of *Pinus sylvestris* L. from 11 regions (countries) across Europe were
190 surveyed by partners in the GenTree consortium (http://www.gentree-h2020.eu/; Opgenoorth
191 et al., 2021) (Fig. 1; Appendix A. Fig. S1, Table S1). Populations were selected from across
192 the distribution, representing the range of environmental variation encountered by the species,
193 but excluding heavily managed stands, or those disturbed by intense, very recent and obvious
194 anthropogenic actions. Populations were representative of local environmental conditions,
195 without being dominated by particular extremes, and included populations at the southernmost
196 edge of the distribution (in Spain, Italy and Greece), and populations in the northernmost edge
197 in Fennoscandia (Norway, Sweden and Finland) and the United Kingdom.
198 Except for two sites (Lithuania and Sweden), populations were sampled in local pairs, i.e. two
199 distinct populations across a local gradient (such as elevation, water availability or day length),
200 but with significant potential for gene flow among them based on previous studies. The
201 geographic distances among populations were variable across the distribution, i.e. in southern
202 sites topographic relief allowed strong environmental contrasts over short spatial scales; while
203 in the north large spatial scales were required, particularly in Fennoscandia. However, F_{ST}
204 values (measure of population differentiation due to genetic structure) among populations
205 across the *P. sylvestris* range have been shown to be extremely low (Robledo-Arnuncio et al.,
206 2004; Wachowiak et al., 2014; Pyhäjärvi et al., 2019). Thus, we assumed that our paired
207 populations are likely in gene flow contact based on these studies that demonstrated the lack
208 of genetic structure at local scales.

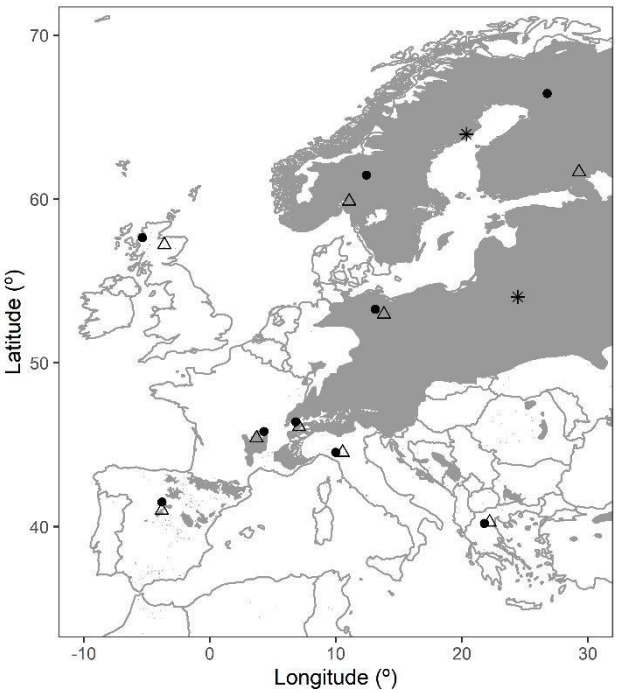

209

210 **Fig. 1.** Location of study populations of *Pinus sylvestris* across Europe. In most regions, pairs
211 of populations located in contrasting conditions were surveyed. Black circles represent the
212 population within a pair that was classed as occupying harsher conditions; triangles represent
213 the population within a pair that was classed as occupying milder conditions, asterisks represent
214 unpaired locations. Grey area represents the species distribution obtained from EUFORGEN
215 (www.euforgen.org).

216

217 We classified each population within the local gradient (pair); distinguishing each as being
218 under milder (M) vs. harsher (H) conditions (Fig. 1, Table S1). Local gradient selection sought
219 contrasting conditions, but was not defined *a priori* by concepts of relative environmental
220 suitability. Therefore, we combined two methods to achieve a robust classification: a climate-
221 based criterion, which coarsely defines suitability based on the climatic space of the species
222 distribution, and a tree-centric criterion based on tree performance (secondary growth data).
223 The latter determined which population within a pair performed better and we accordingly
224 assigned this as the milder (M) site (Anderegg & HilleRisLambers, 2019).

225 We assessed the climatic space of the species by retrieving from CHELSA V1.2 (Karger et al.,
226 2017a, b) the mean annual temperature (T) and annual precipitation (P) of each location
227 obtained from the high-resolution tree occurrence records from the EU-Forest dataset (Mauri

et al., 2017). We then defined density levels of *P. sylvestris* occurrence using a two-dimensional Kernel density estimate, and re-scaled the density levels to the probability density (between 0 and 1) and positioned the paired populations within the climate space. We assumed that the population under harsher conditions was the one with lower probability density, i.e. the population within a pair whose climatic conditions were less frequent within the entire distribution (Fig. 2a). With this criterion, some paired populations had similar density levels and could not be differentiated (i.e. Norwegian and Italian pairs).

In addition, we obtained the tree-ring width series (2006-2015) of surveyed trees from Martínez-Sancho et al. (2019, 2020). We selected the last 10 years when the competitive environment was closer to the sampling year (Anderegg & HilleRisLambers, 2019). We transformed tree-ring widths into annual basal area increments (BAI) using the *dplR* R package (Bunn et al., 2016), which is a better estimate of the overall tree growth than raw data (Biondi & Qeadan, 2008), and averaged the annual figures to get the mean $BAI_{2006\text{-}2015}$ for each tree. Then, we compared mean $BAI_{2006\text{-}2015}$ of paired populations using the *t-test*, after estimating age-, size- and local competition standardised growth values (Anderegg & HilleRisLambers, 2019), i.e. we used the residuals from the relationship $\log(\text{mean}BAI_{1985\text{-}2015}) \sim \text{DBH} + \text{tree age} + \text{CI}$ (Fig. 2b). *CI* is the competition index assessed at the tree level, which describes the competitive environment (see details in the following section *Environmental data*). Mean growth was significantly different for German and Finnish populations. For the rest, mean growth differences were more subtle but matched the classification derived from the climate-based criterion. The only exception was the Spanish pair, where the population with harsher climatic conditions performed slightly better, indicating that climate may not be the sole driver of environmental suitability here.

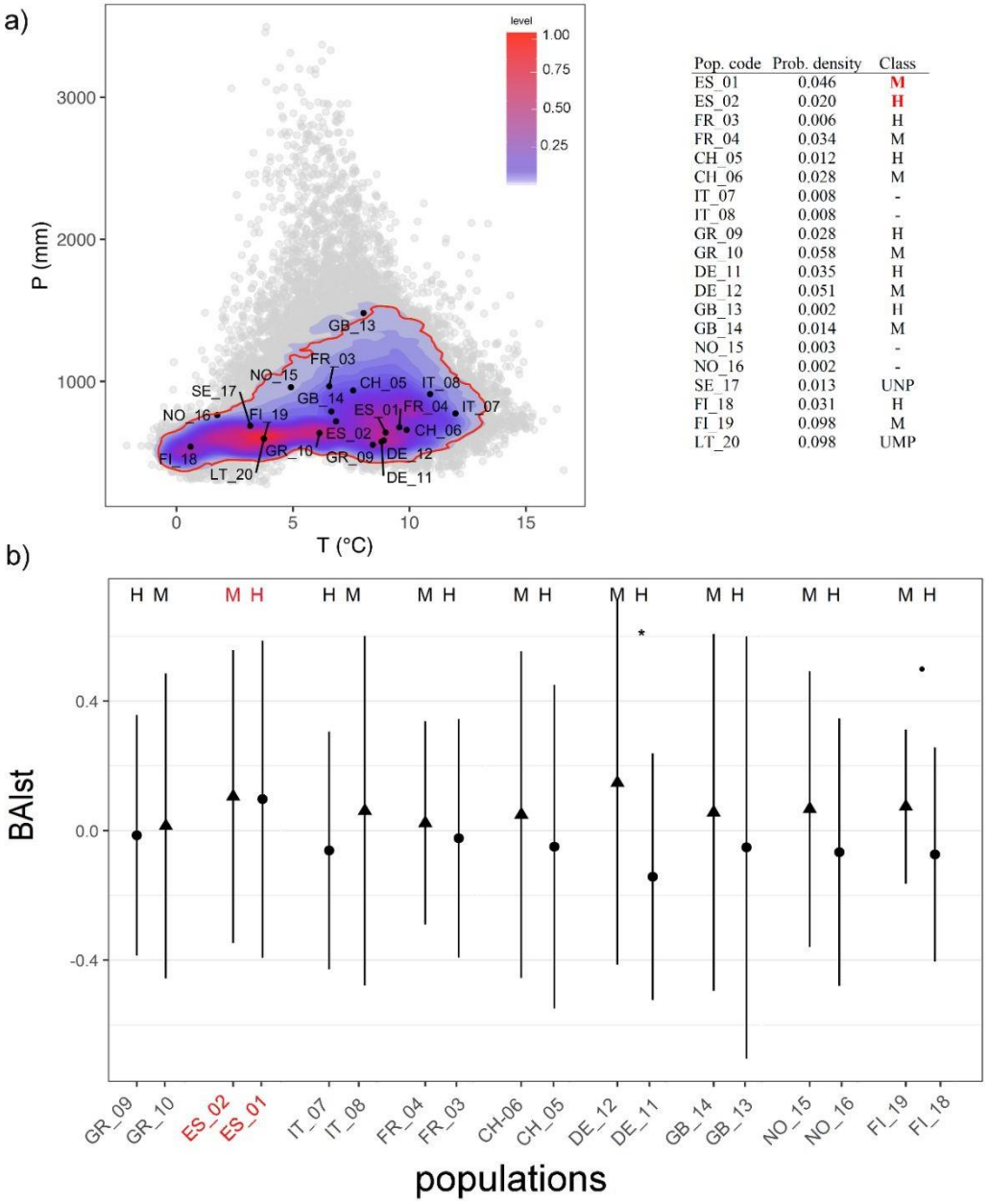

Pop. code	Prob. density	Class
ES_01	0.046	M
ES_02	0.020	H
FR_03	0.006	H
FR_04	0.034	M
CH_05	0.012	H
CH_06	0.028	M
IT_07	0.008	-
IT_08	0.008	-
GR_09	0.028	H
GR_10	0.058	M
DE_11	0.035	H
DE_12	0.051	M
GB_13	0.002	H
GB_14	0.014	M
NO_15	0.003	-
NO_16	0.002	-
SE_17	0.013	UNP
FI_18	0.031	H
FI_19	0.098	M
LT_20	0.098	UMP

Fig. 2. a) Distribution in a climatic space of occurrence data (grey points obtained from Mauri et al., 2017) of *Pinus sylvestris* across Europe using 2D kernel density estimates to define the probability density. Red line contains 95% of the observations. The probability density of each population in the climatic space is shown in the table on the right, and determines the classification within pairs, assigning M (populations under more suitable conditions) to those located in a climate with a higher probability density of occurrence, and H (populations under harsher conditions) to those with smaller probability density of occurrence. b) Mean basal area increments -BAIst- (and standard deviation) standardised by age, size and competitive environment (unitless) of each population (x axis, ordered by latitude) for the period 2006-2015. Triangles represent the higher values within pairs (populations under more suitable

conditions, M), and circles the lower values (populations within pair under harsher conditions, H). Populations in red represent a classification mismatch between both criteria.

Field sampling and trait collection

Within each population, at least 25 adult trees were randomly selected and georeferenced, totalling 511 trees. Selected trees were dominant or co-dominant, healthy, and at least 30 m from the next selected tree (Opgenoorth et al., 2021). We chose ten of the most commonly used plant traits (Table 1) from three trait dimensions important to define the global plant spectrum (Díaz et al., 2016) in order to capture comprehensive species' responses across the distribution (Westoby & Wright, 2006). The three trait dimensions included plant size, which reflects the ability to pre-empt light resources and disperse seeds; stem traits related to hydraulic safety and plant protection; and leaf traits, which balances the acquisition and conservation of resources, i.e. construction costs and growth potential (Wright et al., 2004; Chave et al., 2009; Díaz et al., 2016).

Specifically, in the field we measured tree height (H, m); diameter at breast height (DBH, cm); crown size, calculated with two perpendicular diameters of the crown projection (CP, m^2); bark thickness (Brk, mm), as the average of three to five measurements using a bark thickness gauge (Haglöf Barktax, Sweden); and trunk straightness (TSt) following the scale: 1) moderate or strong bends, 2) slight to moderate bend in different directions, 3) fairly straight (in one direction slightly crooked) and 4) absolutely straight (Opgenoorth et al., 2020). In addition, one wood core was extracted at breast height (1.3 m), perpendicular to the slope direction to avoid reaction wood, to assess wood density (WD, g/cm^3) (Martínez-Sancho et al., 2019, 2020) and one branch from the top of the crown to assess leaf traits (Benavides et al., 2021). For the latter, we collected ten needles of the last complete growing season from each branch (totalling 5110 needles), scanned them and measured their projected area (LA, mm^2) using WinFOLIA (Regent Instruments Inc., Canada), considered a proxy of the total leaf area (Pérez-Harguindeguy et al., 2013). They were then oven-dried at 60 °C for 72 h and weighed for dry

mass, and we estimated specific leaf area (SLA, $mm^2\ mg^{-1}$). We obtained leaf morphological trait per tree averaging the figures of the ten individual needles (Benavides et al., 2020).

Table 1. Overview of functional traits measured in each individual.

	Trait	Units	Trait description	Trait functions
Plant size traits	Height (H)	m	Distance from the soil surface to the top end of the crown	Competitive vigour to capture light, competing either in the vertical or horizontal plane
	Diameter at breast height (DBH)	cm	Diameter of the stem at breast height	
	Crown projection area (CP)	m^2	Area estimation of the crown projection, assuming elliptical areas and using two perpendicular diameters of the crown	
Stem traits	Bark thickness (Brk)	mm	Average of 3-5 measures of bark thickness using a bark gauge	Cambium protection and mechanical support
	Trunk straightness (TSt)	unitless	Categorical variable, from 1 to 4 meaning absolutely straight	Competitive vigour to capture light and mechanical support
	Wood density (WD)	$g\ cm^{-3}$	Ratio of wood dry mass (g) per displaced volume (cm^3)	Mechanical resistance, water storage in the trunk, hydraulic safety, growth-survival trade-off
Leaf traits	N content	%	N concentration in leaf	Trade-offs between investment in support and photosynthetic structures
	Specific leaf area (SLA)	$mm^2\ mg^{-1}$	Ratio between leaf area* and dry mass	
	Leaf area (LA)	mm^2	One-side leaf lamina area*	Gas exchange
	$\delta^{13}C$	‰	Ratio of stable isotopes 13C:12C, reported in parts per thousand (per mil, ‰)	Water use efficiency

* In this study projected leaf area is used.

Finally, for a subset of at least 14 individuals in each population (284 in total), dried needles were ground and analysed for nitrogen content (LNC; %) and isotope ^{13}C content in plant material ($\delta^{13}C$, reported relative to V-PDB, ‰). Leaf collection, storage, processing and morphological trait measurement followed Pérez-Harguindeguy et al. (2013), while the chemical analyses were carried out using gas chromatography-combustion isotope ratio mass spectrometry (GC-C-IRMS) at the UC Davis Stable Isotope Facility

301 (https://stableisotopefacility.ucdavis.edu/) (Benavides et al., 2020, 21). Two of the leaf traits,
302 SLA and LNC, are directly related to the leaf economics spectrum (acquisition and
303 conservation of resources trade-off), while the other two, LA and $\delta^{13}C$, reflect aspects related

to gas exchange in leaves and water use efficiency, respectively. Finally, we also compiled tree age data from Martínez-Sancho et al. (2019, 2020).

Environmental data

At different spatial scales, we selected environmental variables relevant for tree performance (Opgenoorth et al., 2020). At the population scale, 26 climatic variables were retrieved from CHELSA (resolution 30 arcsec, c.a. 1 km^2); and 16 topographic variables derived from the European digital elevation model with 25 m spatial resolution (EU-DEM v. 1.1 from the Copernicus program; https://land.copernicus.eu/).

Moreover, we estimated a competition index (CI) at the tree level (Lorimer, 1983), which represents the degree of competition for available resources with surrounding neighbours. It was calculated using the five nearest trees within a maximum radius of 15 m around each surveyed tree as $CI = \sum_{i=1}^{5} (dbh_i / dbh) / dist_i$, where dbh is the diameter at breast height of the subject tree, dbh_i the diameter at breast height of the competitor tree *i* and $dist_i$ the distance between the subject tree and competitor tree *i*. This index assumes that the net effects of neighbouring trees vary as a direct function of the size of the neighbours and as an inverse function of the distance.

Statistical analyses

We explored changes in the phenotypic space of *P. sylvestris*, analysing trait shifts and drivers across scales, and implemented a multi-level approach to phenotypic integration (*sensu* Armbruster et al., 2014; Klingenberg, 2014) analysing the trait covariation structure across scales within its distribution.

Trait variance partitioning and factors affecting trait variation

First, we ran linear random models for each trait to examine the distribution of the variance of

each trait across scales (Zuur et al., 2009). We included *population* as a random effect that

accounts for the variability among populations, representing the residual variance the variability within populations. We repeated the analysis with *pair* nested within *region* (country) for those populations sampled in pairs to partition the variability among populations driven by the local gradient. Trait values were Box-Cox transformed (including log-transformation as a particular case of Box-Cox transformation), as appropriate, to optimise normality of the residuals.

Next, we tested the effect of environmental factors on trait values (eq. 1). Previously, we ran two principal component (PCAs) and correlation analyses, one for climatic and another for topographic variables, to select those variables that orthogonally explained more variance (Appendix A, Figs. S2, S3; Tables S2, S3). The final selection included mean annual temperature (T, ºC); annual precipitation (P, mm); temperature of the wettest quarter (Twet, ºC), potential total solar radiation (rad, GJ m^{-2}), which varied among populations; slope (sl, º); tree age (years), which varied both among and within populations; and the competition index (CI), for which more than 75% of the variance was within populations (Appendix A, Fig. S4). We also included the quadratic term of T to consider a common non-monotonic response typical of physiological processes along the thermal gradient.

$$Trait \sim age + CI + sl + rad + T + T^2 + P + Twet + (1|population) \quad \text{(eq1)}$$

We fitted all possible linear mixed models (eq. 1) for each trait, and ranked them using the Akaike Information Criterion (AIC), where 'better' models achieved an improvement of at least two units AIC over the next one (Burnham & Anderson, 2002), and followed the principle of parsimony to prioritise the simplest model (Appendix C, Table S4). We assessed the significance of factors by comparing models with and without each factor selected in the best model using the *likelihood ratio test* (Zuur et al., 2009).

Trait covariation across gradients

Then, we characterised overall and intrapopulation structures of trait covariation and analysed its variation across the local (mild *vs*. harsh) and rangewide (climate) gradients. Previous

356 analyses showed an important effect of tree age on size plant and stem traits (Table 2). Thus,
357 we removed the effect of age prior to trait covariation analysis by using the residuals from the
358 relationship between each trait and age (trait ~ age). In doing so, we accounted for the potential
359 confounding effect of ontogeny on covariation patterns. Then, we obtained the trait correlation
360 matrices with Pearson correlation analyses (except for trunk straightness, for which we used
361 Spearman correlations, as it is an ordinal variable). We used permutation tests to evaluate the
362 statistical significance of each pairwise correlation at the population and species levels. Traits
363 within individuals were untied and shuffled 1000 times. From each randomisation, we assessed
364 pairwise trait correlations, generating a null distribution, and we extracted a p-value associated
365 with the observed correlations. At the species level (i.e. with pooled data), in each
366 randomisation, traits from 25 individuals (instead of the complete sample size, i.e. > 500) were
367 extracted to generate the null distribution and get significant coefficients comparable to those
368 obtained at the population level. Moreover, very small, meaningless but highly significant
369 correlation coefficients, typically obtained from large-sized samples, were discarded
370 (Aggarwal & Ranganathan, 2016). Thus, all significant pairwise correlations (significantly
371 stronger from what is expected by chance) had values over $|\rho| \geq 0.3$. We graphically represented
372 the covariation structures running a network analysis with the correlation coefficients for each
373 population. We generated undirected circle networks, with traits as nodes, and the significant
374 correlations amongst them as edges.
375 Next, we calculated two quantitative measures of trait covariation degree, i.e. the *edge density*
376 (ED), assessed as the ratio between the number of significant correlations (edges) and all
377 possible pairwise trait combinations, and the *functional variability shape* (FS) (*sensu* Boucher
378 et al 2013), i.e. the variance of the eigenvalues of the trait correlation matrix which considered
379 a phenotypic integration index (Wagner, 1984; Cheverud et al., 1989). If traits are uncorrelated
380 within populations, eigenvalues will be similar and have low variance, while eigenvalues will
381 show high variance when traits are correlated (Dwyer & Laughlin, 2017b). Finally, we fitted

linear models to analyse the effects of the climate (T, T^2, P and Twet) and the local gradient (H vs M) on these two metrics. We fitted all possible models, ranked them using the Akaike Information Criterion corrected for small sample size (AICc), and assessed the significance of selected factors by comparing the model with and without factors selected in the optimal model using the *likelihood ratio test* (Zeileis & Hothorn, 2002).We also explored ED and FS variation across latitude (see Supporting Information).

All statistical analyses were performed in R (version 3.6.1, R Core Team, 2019), using the *stats* package for correlation analysis and linear models, *lme4* package (Bates et al., 2015) and MuMIn (Barton, 2020) for linear mixed models, *lmtest* package for likelihood ratio test in linear models (Zeileis & Hothorn, 2002), *AID* package for Box-Cox transformation (Asar et al., 2017), *igraph* package (Csardi & Nepusz, 2006) for the network analysis, and *ggplot2* package (Wickham, 2016) for graphics.

RESULTS

Distribution of trait variation

Trait values varied not only across regions but also between pairs and within populations (Fig. 3; Appendix B, Fig. S5). Plant size traits were the most variable with the highest coefficients of variation (Fig. 3), while WD and leaf isotopic signature were the most stable traits.

The distribution of trait variance was also trait-dependent (Fig. 3). Plant size differed more among populations (over 60% of trait variance for the three traits) than within populations, leaf traits varied similarly at both scales (among and within populations), while stem traits had higher variance within populations that among them. All traits showed non-negligible variance between pairs (at local gradients), except for $\delta^{13}C$ (Fig. 3).

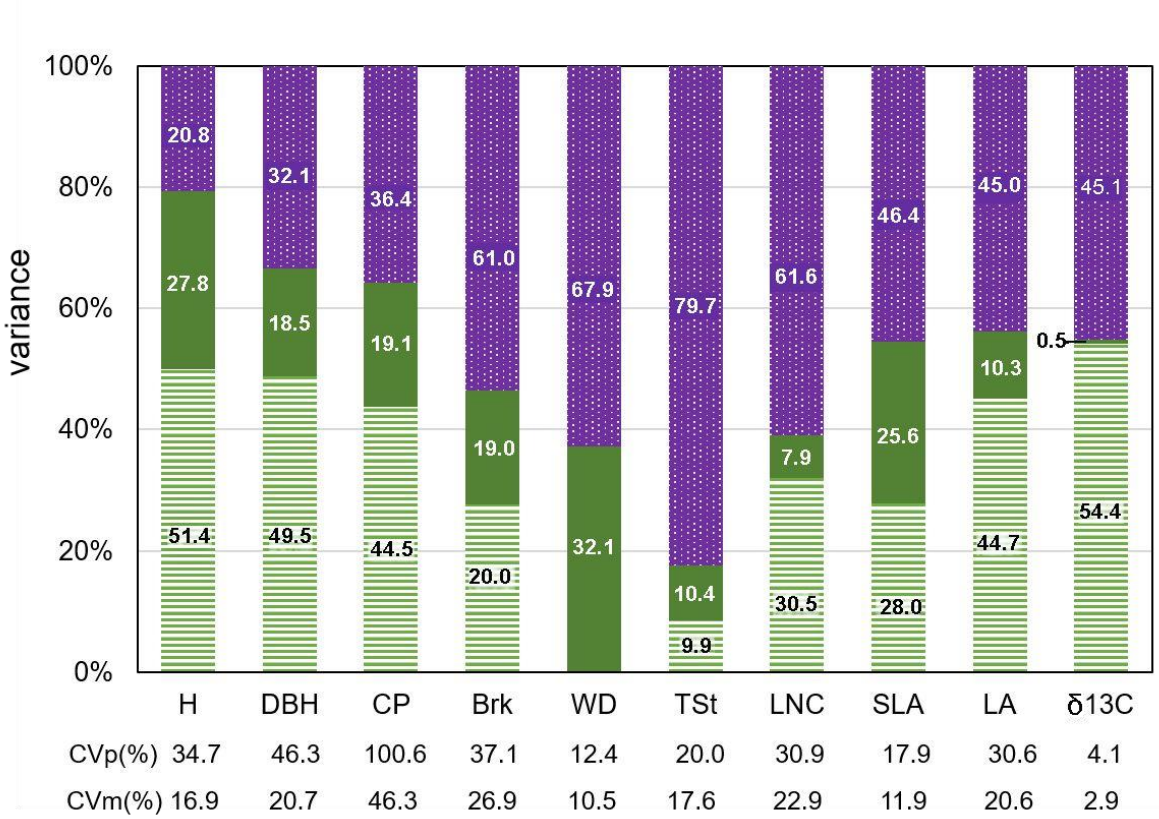

Fig. 3. Distribution of trait variability. The partitioning of variance revealed the component within populations (dotted purple bar) and among populations (green bars), which in turn can be partitioned into variance among regions (green striped bars) and paired populations in a local gradient (solid green bars). The coefficients of variation (CV with pooled data, CVm within-population mean) of each trait are shown. H: tree height, DBH: diameter at breast height, CP: crown projection size, Brk: bark thickness, WD: wood density, TSt: trunk straightness, LNC: leaf N content, SLA: specific leaf area, LA: leaf area, δ13C: isotopic signature of ^{13}C. Variance partitioning analysis was performed on both raw and transformed data, which resulted in very close outcomes. This figure shows the results only obtained with raw data.

Similarly to trait variance partitioning, linear models showed that there are factors acting on trait means at different scales (Table 2; Fig. 4; Appendix B Figs. S4, S6). Age and competition (CI) significantly affected traits at the tree level, accounting for variance within populations for stem and plant size traits (Table 2). We also found a significant climatic signal for all traits except for trunk straightness and SLA (Table 2; Figs. 4, S6), with a non-linear effect of mean annual temperature on plant size, stem and leaf traits. They all presented lower means at both

edges, and the highest value in the centre-warmer half of the thermal range (Figs. 4, S6). Moreover, the mean temperature in the wettest quarter of the year had a positive effect on H, while precipitation had a negative effect on H and LA. Potential solar radiation derived from the topography had a positive effect on $\delta^{13}C$, Brk and LNC, but a negative effect on WD (Table 2).

Integration of traits along gradients

Both metrics, edge density (ED) and functional variability shape (FS), were correlated in our study populations ($\rho = 0.67$), showing the same trends. Considering all populations, the phenotypic space of *P. sylvestris* was poorly coordinated, with an edge density of only 6.67% and functional variability shape of 0.49 (Appendix B, Fig. S7). Only three traits covaried (DBH, CP and Brk), three pairwise correlations that appeared in most of the populations (Fig. 5, Fig. S8). However, this figure increased when we calculated ED within each population, ranging from 17.8% up to 63.9% (FS from 0.62 to 2.2). This range reflected important differences in the trait correlation structure that differed not only quantitatively (number of significant correlations) (Fig. 5), but also qualitatively (traits more frequently involved in trait covariations) (Fig. S8). In fact, only six trait pairs were frequently correlated and showed a mean correlation coefficient over $|\rho| > 0.3$ (significance threshold), namely correlations between DBH and CP, Brk and H, between CP and Brk, and between SLA and $\delta^{13}C$ and LA. The variation of edge density and functional variability shape across the rangewide climatic gradient (and latitudinal) showed significantly greater values in northern populations where conditions were cooler (significance levels $p<0.01$ for T (ED and FS), $p<0.1$ for T^2 (ED), Fig. 6; see Fig. S9 results in terms of latitude). This asymmetry was nonetheless driven by the values obtained in the northernmost population in Finland, diminishing the effect of temperature or latitude when this population was omitted (Appendix B, Fig. S10). Moreover, we found a significant effect of the local gradient with consistently higher trait covariation in populations

449 under harsher conditions (estimated marginal means ED=29.9%, log(FS)= -0.0173) compared
450 to those under milder conditions (estimated marginal mean ED=21.5%, log(FS)= -0.2186)
451 ($p<0.05$ for ED and $p<0.1$ for FS, Fig. 6). We did not find a significant interaction among the
452 local gradient and mean annual temperature (or latitude).

Table 2. Summary of the optimal linear mixed models for individual trait values. Estimates (standard errors) and significance assessed with likelihood-ratio tests are shown.

		Age	CI	slope	rad	T	T^2	P	Twet	n	R^2m	R^2c
Plant size traits	H	0.025*** (0.005)				4.417*** (1.061)	-0.338*** (0.008)	-0.017*** (0.004)	0.375*** (0.152)	495	0.53	0.80
	log(DBH)	0.003*** (0.0003)	-0.204*** (0.189)			0.264*** (0.060)	-0.018*** (0.080)			497	0.54	0.79
	log (CP)	0.005*** (0.0007)	-0.456*** (0.044)	-0.014** (0.004)		0.543*** (0.131)	-0.034** (0.010)			497	0.49	0.75
Stem traits	BxCx (Brk)	0.010*** (0.002)	-0.514*** (0.122)		0.378. (0.2100)	0.707** (0.257)	-0.044* (0.020)			497	0.30	0.53
	BxCx (WD)	0.001** (0.004)		-0.006** (0.002)	-0.088* (0.038)	0.029* (0.012)				365	0.14	0.31
	TSt	-0.004*** (0.001)								497	0.05	0.24
Leaf traits	BxCx (LNC)				(0.057*)	(0.023*)	-(0.0074)**			277	0.28	0.43
	log (SLA)		(0.012*)							497	0.01	0.54
	log (LA)		(0.105)		(0.183)	(0.0413) 0.186***	(0.003) -0.010**	(0.0002) -0.0004**		497 277	0.39 0.06	0.56 0.51
	$\delta^{13}C$		-0.262*		0.350.							

CI: competition index; slope (º); rad: potential total solar radiation (GJ/m²); T: mean annual temperature (ºC); P: mean annual precipitation (mm); Twet: temperature of the wettest quarter of the year (ºC) ; H: tree height; DBH: diameter at breast height; CP: crown projection area; Brk: bark thickness; TSt: trunk straightness; WD: wood density; LNC: leaf N content; SLA: specific leaf area; LA: leaf area; δ13C (‰). ΔAIC represents the improvement of the model removing non-significant variables compared to the saturated model. Marginal (R^2m) and conditional (R^2c) r-squared are shown, showing the variance explained by the model considering only fixed and both fixed and random effects. Significance: •10%, *5%, **1%, ***01%.

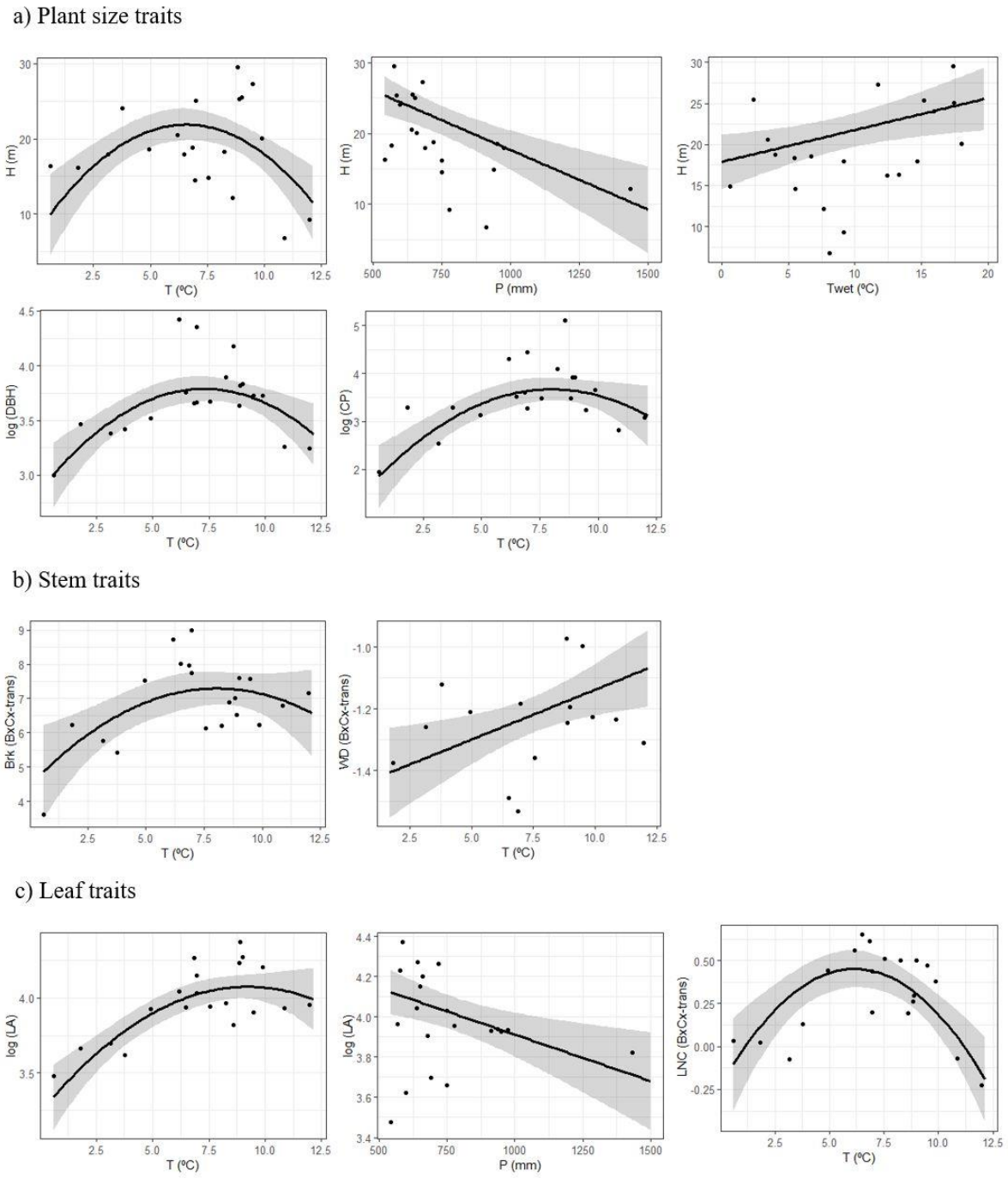

Fig. 4. Traits versus climatic variables. Plots show linear mixed models as described in Table 2, and selected according to AIC and parsimony criteria**.** a) Traits related to plant size, b) stem traits, and c) leaf traits. Only significant effects are shown. T: mean annual temperature (ºC), P: mean annual precipitation (mm), Twet: temperature of the wettest quarter (ºC), H: height (m), DBH: diameter at breast height (cm), CP: crown projection area (m^2), Brk: bark thickness (mm), WD: wood density (g cm^{-3}), d13C (‰), LNC: leaf N content (%), LA: leaf projected area (mm^2). Grey area represents the 95% confident intervals, which reflect only the variance of the fixed effects, not the random effects (populations), and points indicate population means (see Fig. S6 with tree level observations).

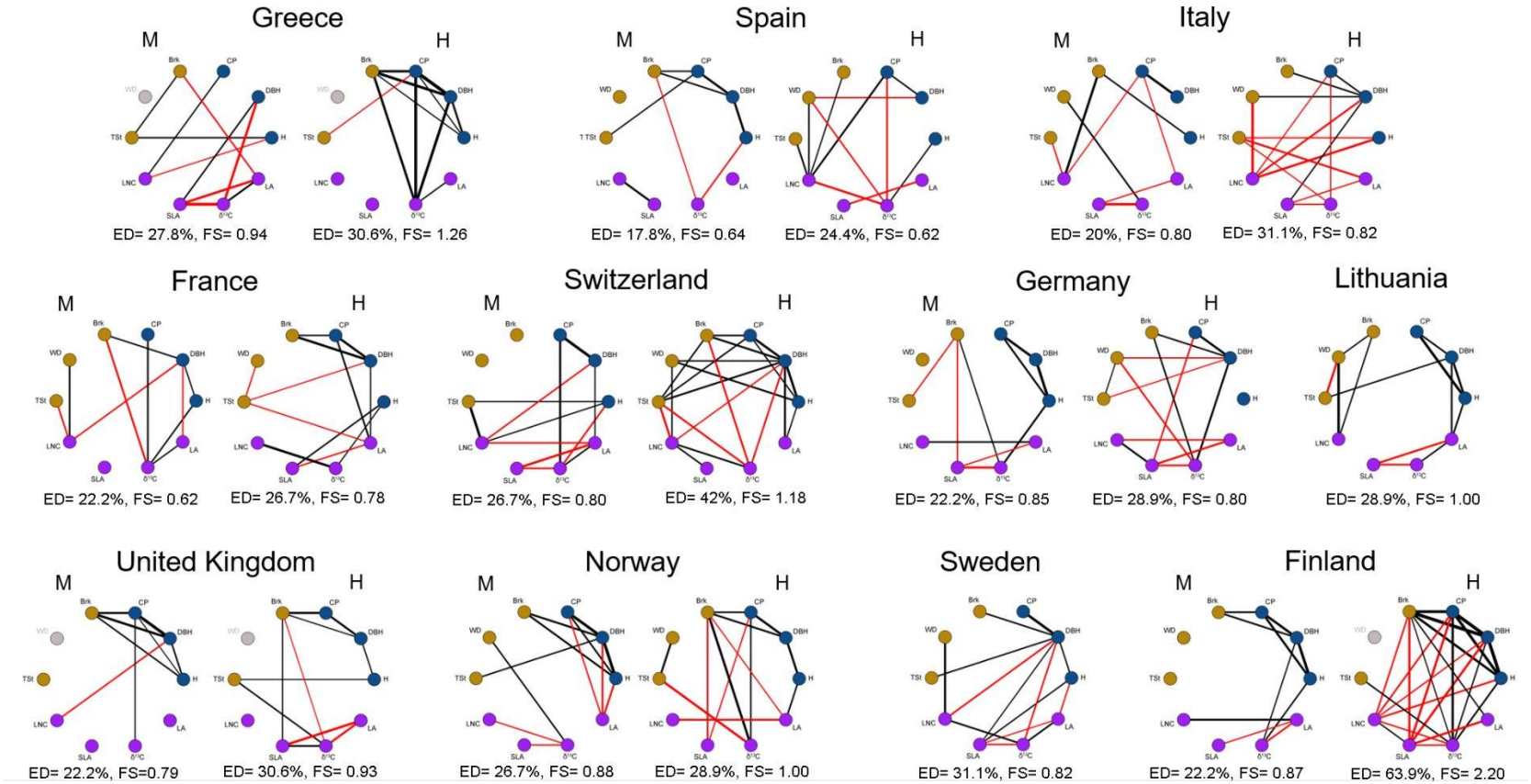

Fig. 5. Trait correlation networks in 20 *Pinus sylvestris* populations across 11 regions. Traits belong to three dimensions: plant size (blue), stem traits (brown) and leaf traits (purple). Local gradient is given as M (milder environment) vs H (harsher environment). Black lines represent positive correlations, while red ones are negative. Line colour intensity shows the strength of the correlation. H: tree height, DBH: diameter at breast height, CP: crown projection area, Brk: bark thickness, TSt: trunk straightness, WD: wood density, LNC: leaf N content, SLA: specific leaf area, $\delta^{13}C$: isotopic signature of ^{13}C, LA: leaf area. Where 'WD' is given in light grey means that we lack this trait in those populations. Plant size and stem traits were standardised by age before the correlation analysis. Correlation analyses were conducted with data surveyed in 25 trees per population.

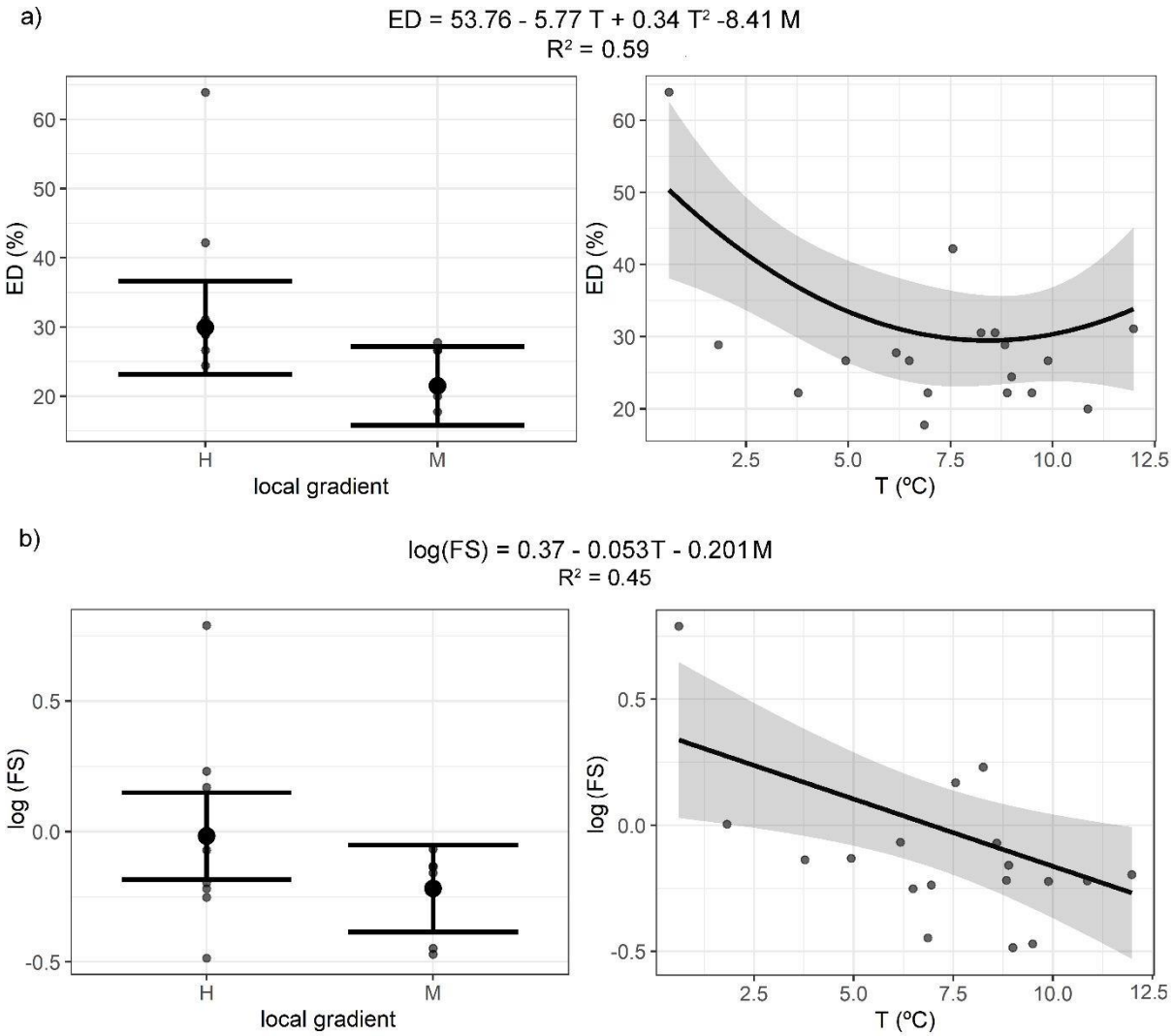

Fig. 6. Effect of local gradient and mean annual temperature (T) on a) edge density (ED); and on b) (log) functional variability shape (FS). ED is the ratio between the number of significant correlations and all possible pairwise trait combinations, and FS is the variance of the eigenvalues of the trait correlation matrix. On the top, the expression of the optimal models and their R^2. Whiskers and grey areas represent the 95% confidence intervals. Points represent the observed values. M: populations under milder conditions; H: populations under harsher conditions.

DISCUSSION

Phenotypic variation within the widely distributed conifer *Pinus sylvestris* has an important intrapopulation component that, irrespective of other factors such as genetic variability among

491 individuals or differences in their microhabitat, was significantly driven by ontogeny (age) and
492 competition with neighbours. At the interpopulation level, temperature strongly influenced
493 mean trait values, with non-linear effects that showed smaller trees with smaller and less
494 productive (less N content) needles at both edges of the thermal range of the distribution, i.e.
495 close to the southern and northern edges of the distribution. We also found a systematically
496 higher degree of trait covariation (higher statistical phenotypic integration) in populations
497 under harsher conditions in local gradients, and an increasing trend at the northern edge of the
498 distribution, which showed that integration varies at different spatial scales (Fig. 6). Despite
499 finding qualitative differences among populations without same patterns in covarying traits,
500 the consistently higher trait covariation under harsher conditions across the distribution,
501 entailing 'tighter' phenotypes, suggests that it has an adaptive value.
502
503 **Trait covariation across local gradients**
504 At the beginning of this century, the concept of plasticity of integration was coined (Murren,
505 2002; Pigliucci, 2003; Piggliucci, 2004), recognising that, as for individual traits, trait
506 correlation could vary dramatically in response to environment or spatial scale (Schlichting,
507 1986; Nicotra et al., 1997; Anderegg et al., 2018; Rosas et al., 2019). In fact, some experimental
508 studies connected stress to 'tighter' phenotypes probably seeking higher coherence or
509 optimality under adverse conditions (Schlichting, 1986; 1989; Chapin, 1991; Gianoli, 2004;
510 Damián et al., 2020, but see Pigliucci & Kolodynska, 2002a,b; Pigliucci & Kolodynska, 2006).
511 Our sampling design, with population pairs assumed to be genetically connected due to spatial
512 proximity and highly efficient long-distance gene flow by wind dispersion (a robust assumption
513 given the many studies on the topic in this widely studied species, e.g. Robledo-Arnuncio et
514 al., 2004; Wachowiak et al., 2014; Pyhäjärvi et al., 2019), drew outcomes in agreement with
515 the expected positive relationship between level of stress and phenotypic coordination. High
516 levels of gene flow between paired populations mean that both share a common gene pool, and

517 so divergence in trait means can be assumed to reflect differences in local adaptive pressures
518 (Conner & Hartl, 2004; Holderegger et al., 2006). Therefore, the increasing edge density and
519 functional variability shape in harsher conditions suggest that trait covariation responds to
520 different environments. It is remarkable that this pattern is found across the entire distribution,
521 between paired populations subjected to different gradients (elevation, water availability, day
522 length), and is a strong indication that higher trait covariation may be adaptive, in accordance
523 with recent work exploring covariation in leaf traits (Damián et al., 2020). In other words,
524 'tighter' phenotypes appear in more stressful sites to avoid the high cost of maintaining certain
525 and rare trait combinations (Westoby & Wright, 2006; Dywer & Laughlin, 2017a). However,
526 our study lacks the means to discern the underlying mechanism, i.e. whether these 'tighter'
527 phenotypes are expressing local adaptation (Conner & Hartl, 2004; Kawecki & Ebert, 2004) or
528 adaptive plasticity is operating (Pigliucci, 2001; Stamp & Hadfield, 2020). Regardless, the
529 consistency and robustness of this pattern across contrasting climatic conditions and selective
530 pressures clearly suggest an adaptive value for trait covariation in this species (Damián et al.,
531 2020).
532
533 **Rangewide trait covariation**
534 We hypothesised that the pattern of response to stress at relatively small spatial scales might
535 also occur at larger scales among climatically different regions. We based this on the central-
536 periphery hypothesis (Soulé, 1973; Albeli et al., 2014) that suggests that at the extreme edges
537 of a species distribution, the number of trait combinations should be limited (higher trait
538 covariation) due to the high cost of certain values, resulting in more integrated phenotypes
539 (Westoby & Wright, 2006; Dywer & Laughlin, 2017a). It is notable that connection between
540 increasing trait covariation with stress has not always been captured (Pigliucci & Kolodynska,
541 2002a, b; 2006; Bouchar et al., 2013), showing the complexity of the effect. Our results showed
542 a greater trait covariation at the northern edge of the species distribution (cold edge) supporting

apparently our hypothesis (Fig. 6). However, this outcome should be taken with caution as this latitudinal and climatic pattern is mainly driven by the trait covariation obtained in the northernmost population in Finland (Table S1; Fig. S10). Whether these values represent outliers or the threshold that triggers higher coordination of traits would need further investigation with more surveys in peripheral populations.

At the warm (southern) edge we did not find this increasing pattern opposing our expected positive relationship between phenotypic integration and less suitable conditions at the margins (Fig. 6a). Trait covariation is considered to be a trade-off between adaptation and constraints (Pigliucci, 2003; Merilä & Björklund, 2004). As previously mentioned, natural selection may favour certain combinations of traits and, therefore, trait coordination can be adaptive (Damián et al., 2020). However, certain relationships among traits may limit their plasticity (Gianoli & Palacio-López, 2009) becoming a threat for adaptation under unpredictable conditions (Jernigan et al., 1994). In Mediterranean mountains, the climate frequently encompasses extreme events of summer drought and cold winters (Pereira & Chaves, 1995), hence populations should have a higher disposition for phenotypic integration (Dwyer & Laughlin, 2017a; Michelaki et al.,2019) compared to those thriving on summer drought-free, more benign areas (Baraloto et al.,2010; Fortunel et al., 2012). However, the unpredictable nature of the Mediterranean climate and a complex topography, which creates a high heterogeneity of environmental conditions over short distances, can underlie lower trait covariation than expected, where trait covariation can be considered a disadvantage rather than a benefit (Jernigan et al., 1994). Also, our southern populations belong to fragmented areas of the distribution southern edge (Fig. 1). This means that they could be affected by pernicious effects related to both genetic drift and genetic isolation, which may in turn cause a selection inefficiency (Sexton et al., 2009). In contrast, northern populations lie environmentally closer to the centre of the distribution and likely have much larger population sizes. Consequently,

568 they may exhibit better responses to natural selection (Kirkpatrick & Barton, 1997), producing
569 more 'optimised' phenotypes based on higher degree of trait covariation (Bouchar et al., 2013).
570
571 **Trait variation across environmental gradients**
572 Most of the trait clines showed a very similar pattern across the species distribution (Fig. 4; Fig
573 S6). In particular, we detected non-linear responses along the temperature gradient that reflects
574 lower climatic suitability at both edges of the range, which translated into bigger trees with
575 larger and more nutrient-rich needles in the central-warmer part of the range (central Europe).
576 At the northern edge, *P. sylvestris* is normally limited by low temperatures and a shorter length
577 of the growing season; while at the southern edge, it is mainly limited by a combination of high
578 summer temperature and drought (Carlisle & Brown, 1968; Castro et al., 2004). In our study
579 populations, the pattern along the thermal range matched expectations: shorter trees with
580 smaller leaves with lower nutrient content at both extremes (Reich et al., 2014; Wright et al.
581 2017). In parallel, the precipitation range translated into wetter locations being less suitable,
582 with decreasing tree size and smaller leaf area. This trend was mainly driven by trait values in
583 populations in Scotland, which represents the north-western edge of the range. There, *P.*
584 *sylvestris* populations are considered to be in long-term decline, preceding human influence
585 (Bennet et al., 1984), which is thought to be partially due to increasing precipitation leading to
586 the formation of bogs.
587 Traits related to plant size were most tightly correlated throughout the range; and they also
588 correlated with bark thickness, which agrees with previous work in two populations of *P.*
589 *sylvestris* (Carvalho et al., 2020). Allometric constraints determine that taller trees normally
590 have a thicker trunk and larger crown, associated with thicker bark that confers higher
591 mechanical support and defence (Niklas, 1999; Paine et al., 2010). Among the leaf traits, the
592 most widespread covariations were the negative correlations between SLA and LA and
593 between SLA and $\delta^{13}C$. The latter was also found in Carvalho et al. (2020) and reflects that

individuals investing more in long-lasting, larger and denser needle tissue (lower SLA) have higher water use efficiency. The leaf economic spectrum (LES) describes gradual strategies for plants running from low-cost, short-lived leaves with rapid return of carbon and nutrients (i.e. high SLA and N content) to costly, long-lived leaves with slow returns (low SLA and N content) holding low photosynthetic rates (Wright et al., 2004). However, our data do not fit this pattern, as we found no clear relationship between N content and SLA, outcome that agrees with the different sensitivity to climate shown by both traits in this study and elsewhere (Rosas et al., 2019; Umaña & Swenson, 2019). In addition, we found a negative covariation between SLA and LA, which disagrees with studies showing that larger leaves are normally less dense at the intraspecific level (Martin et al., 2017; Benavides, Scherer-Lorenzen et al., 2019). Variation of leaf size in our climatic gradient followed the global pattern described by Wright et al. (2017), i.e. smaller leaves at higher latitudes and in drier and warmer places. However, SLA is a rather complex trait, especially in evergreens (Lusk et al., 2008). It integrates the trade-off between reduction costs and prolongation of leaf lifespan in resource-limited environments determined by multiple factors, including climate (precipitation, drought or minimum temperatures), light availability or soil characteristics (Wright et al., 2004; Gonzalez-Zurdo et al., 2016; Gong & Gao, 2019). Therefore, this mismatch (the unexpected negative correlation between SLA and LA) may reflect a complex response to different factors or scales involving other associated traits that we did not measured (e.g. leaf thickness, leaf lifespan) (Wilson et al., 1999).

CONCLUSIONS

The multivariate approach to the phenotype, recognising the importance of trait covariation, is emerging as a necessary milestone to comprehend species responses to environmental variation. Here, we analysed the distribution of trait mean and variability across the distribution of the widely distributed *Pinus sylvestris,* and found idiosyncratic covariation structures with

traits covarying differently across scales. More importantly, we found a systematic increase of trait covariation in more stressful sites at a regional scale, suggesting that regardless of the traits involved, there is a pattern towards more coordinated and more efficient responses –'tighter phenotypes'- in such conditions, likely related to adaptive processes.

ACKNOWLEDGEMENTS

We are in debt to all the people collaborating with the field and lab work collecting and assessing data, especially to David López-Quiroga, Antonio Mas, Lenka Slámová and all of our colleagues within the GENTREE. We also thanked Omar Flores for his support with R coding. We are also very thankful to Dr. L. Anderegg, Dr. M. Umaña and three anonymous reviewers for their constructive and useful comments. They have been crucial to reach the final version of this manuscript.

Funding was provided by the European Union Horizon 2020 Project GenTree (Grant Agreement No. 676876). Extra support came from the Spanish projects REMEDINAL TE-CM (Autonomous Community of Madrid, S2018/EMT-4338), Phenotypes (PGC2018-099115-B-100), COMEDIAS (CGL2017-83170-R, Spanish Ministry of Science, Innovation and Universities), and Swiss Secretariat for Education, Research and Innovation (SERI) under contract No. 6.0032. BC was funded by CAPES fellowship (DOC-PLENO - Programa de Doutorado Pleno no Exterior. Grant Agreement No 99999.001266/2015-02, Brazil). RB is now funded by the Contrato-Programa CEEC Individual, Fundação para a Ciência e Tecnologia, Portugal. CCB was supported by a postdoctoral fellowship of the Ramón Areces Foundation.

AUTHORS' CONTRIBUTIONS

RB, FV, BC, AE, SM, EMS conceived the ideas and designed methodology. SC led the selection of sites. RB, BC, CCB, SM, FV, PF collected field data. PF and EMS provided wood density and age data. RB, BC, CCB assessed leaf traits. RB analysed the data, led the writing of the manuscript. All authors contributed significantly with comments to the different versions of the manuscript and gave the approval for publication.

DATA AVAILABILITY

Wood density, tree age (Martínez-Sancho et al. 2019), leaf data (Benavides et al. 2020) and the rest of phenotypic and environmental data (Opgenoorth et al. 2020) are all available in figshare.

SUPPLEMENTARY INFORMATION

Appendix A. Information about the study sites.

Table S1. Description of the study sites

Fig. S1. Variation in mean annual temperature (T), precipitation (P) and mean temperature of the wettest quarter (Twet) of the study populations across latitude

Fig. S2. PCA biplots (left) and loadings (right) based on analysis of data for 26 climatic variables from each population.

Fig. S3. PCA biplot (left) and loadings (right) based on analysis of data for 16 topographic variables from each population.

Table S2. Spearman correlation coefficients among climatic variables in the study sites

Table S3. Spearman correlation coefficients among topographic variables.

Fig. S4. Distribution of trait variance of environmental variables.

Appendix B. Surveyed traits: distribution, mean values and covariation.

Fig. S5. Boxplots of traits in each population, s) plant size and stem traits, b) leaf traits.

Fig. S6. Traits versus climatic variables.

Fig. S7. Trait correlations of *Pinus sylvestris* phenotype.

REFERENCES

Abdala-Roberts, L., Rasmann, S., Berny-Mier, J.C., Covelo, F., Glauser, G. & Moreira, X. (2017). Biotic and abiotic factors associated with altitudinal variation in plant traits and herbivory in a dominant oak species. *American Journal of Botany,* 103, 2070-2078. https://doi.org/10.3732/ajb.1600310.

Aggarwal, R. & Ranganathan, P. (2016). Common pitfalls in statistical analysis: The use of correlation techniques. *Perspectives in Clinical Research*, 7, 187–190. https://doi.org/10.4103/2229-3485.192046

Abeli, T., Gentili, R., Mondoni, A., Orsenigo, S. & Rossi, G. (2014). Effects of marginality on plant population performance. *Journal of Biogeography* 41, 239–249. https://doi.org/10.1111/jbi.12215

Albert, C.H., Thuiller, W., Yoccoz, N.G., Douzet, R., Aubert, S. & Lavorel, S. (2010). A multi-trait approach reveals the structure and the relative importance of intra- vs. interspecific variability in plant traits. *Functional Ecology*, 24, 1192–1201. https://doi.org/10.1111/j.1365-2435.2010.01727.x.

696 Anderegg, L.D.L., Berner, L.T., Badgley, G., Sethi, M.L., Law, B.E. & HilleRisLambers, J.
697 (2018). Within-species patterns challenge our understanding of the leaf economics
698 spectrum. *Ecology Letters*, 21, 734–744. https://doi.org/10.1111/ele.12945.
699 Anderegg, L.D.L. & HilleRisLambers, J. (2019). Local range boundaries vs. large-scale trade-
700 offs: climatic and competitive constraints on tree growth. *Ecology Letters*, 22, 787–796.
701 https://doi.org/10.1111/ele.13236
702 Armbruster, W.S., Pélabon, C., Bolstad, G.H. & Hansen, T.F. (2014). Integrated phenotypes:
703 understanding trait covariation in plants and animals. *Philosophical Transactions of the*
704 *Royal Society B*, 369, 20130245. https://doi.org/10.1098/rstb.2013.0245.
705 Asar, O., Ilk, O. & Dag, O. (2017). Estimating Box-Cox Power Transformation Parameter Via
706 Goodness-of-Fit Tests Communications in Statistics. *Simulation and Computation*, 46, 91-
707 105. https://doi.org/10.1080/03610918.2014.957839.
708 Baraloto, C., Paine, C.E.T., Poorter, L., Beauchene, J., Bonal, D., Domenach, A.M., Hérault,
709 B., Patiño, S., Roggy, J.C., & Chave, J. (2010). Decoupled leaf and stem economics in
710 rain forest trees. *Ecology Letters*, 13, 1338–1347. https://doi.org/10.1111/j.1461-
711 0248.2010.01517.x.
712 Barton, K. (2020). MuMIn: Multi-Model Inference. R package version 1.43.17.
713 https://CRAN.R-project.org/package=MuMIn
714 Bates, D., Maechler, M., Bolker, B. & Walker, S. 2015. Fitting linear mixed-effects models
715 using lme4. *Journal of Statistical Software*, 67, 1-48.
716 https://doi.org/10.18637/jss.v067.i01.
717 Benavides, R., Carvalho, B., Bastias, C.,C. López-Quiroga, D., Mas, A., Cavers, S., Gray, I.,
718 Albet, A., Alía, R., Ambrosio, O., Aravanopoulos, F., Auñón, F., Avanzi, C., Avramidou,
719 E., Bagnoli, F., Ballesteros, E., Barbas, E., Bastien, C., Bernier, F., Bignalet, H. et al.
720 (2020). The GenTree Leaf Collection: Inter- and intraspecific variation of leaf traits in

721 seven forest tree species across Europe. *figshare.*
722 https://doi.org/doi:106084/m9figshare12044370.
723 Benavides, R., Carvalho, B., Bastias, C.C., López-Quiroga, D., Mas, A., Cavers, S., Gray, I.,
724 Albet, A., Alía, R., Ambrosio, O., Aravanopoulos, F., Auñón, F., Avanzi, C., Avramidou,
725 E., Bagnoli, F., Ballesteros, E., Barbas, E., Bastien, C., Bernier, F., Bignalet, H. et al.
726 (2021). The GenTree Leaf Collection: Inter- and intraspecific variation of leaf traits in
727 seven forest tree species across Europe. *Global Ecology and Biogeography* (in press).
728 https://doi.org/10.1111/geb.13239.
729 Benavides, R., Scherer-Lorenzen, M. & Valladares, F. (2019). The functional trait space of tree
730 species is influenced by the species richness of the canopy and the type of forest. *Oikos*,
731 128, 1435-1445. https://doi.org/10.1111/oik.06348.
732 Benavides, R., Valladares, F., Wirth, C., Müller, S. & Scherer-Lorenzen M. (2019).
733 Intraspecific trait variability of trees is related to canopy species richness in European
734 forests. *Perspectives in Plant Ecology, Evolution and Systematics*, 36, 24–32.
735 https://doi.org/10.1016/j.ppees.2018.12.002.
736 Bennett, K.D. (1984). The post-glacial history of *Pinus sylvestris* in the British Isles.
737 Quaternary Science Reviews, 3, 133-155.https://doi.org/10.1016/0277-3791(84)90016-7.
738 Berg, R.L. (1960). The ecological significance of correlation Pleiades. *Evolution*, 14, 171-180.
739 https://doi.org/10.2307/2405824
740 Biondi, F. & Qeadan, F. (2008). A theory-driven approach to tree-ring standardization : defining
741 the biological trend from expected basal area increment. *Tree-Ring Resea*rch, 64,
742 81–96.
743 Bonser, S.P. (2006). Form defining function: Interpreting leaf functional variability in
744 integrated plant phenotypes. *Oikos*, 114, 187–190. https://doi.org/10.1111/j.2006.0030-
745 1299.14425.x.

Boucher, F.C., Thuiller,W., Arnoldi, C., Albert, C.H. & Lavergne, S. (2013). Unravelling the architecture of functional variability in wild populations of *Polygonum viviparum* L. *Functional Ecology*, 27, 382–391. https://doi.org/10.1111/1365-2435.12034

Bunn, A., Korpela, M., Biondi, F., Campelo, F., Mérian, P., Qeadan, F., Zang, C., Buras, A., Cecile, J., Mudelsee, M. & Schulz, M. (2016). dplR: Dendrochronology Program Library in R. R package version 1.6. 9. https://CRAN.R-project.org/package=dplR

Burnham, K.P & Anderson, D.R. (2002). Model selection and multimodel inference a practical information-theoretic approach. 2nd Edition. Springer-Verlag.

Carlisle, A. & Brown, A.H.F. (1968). *Pinus sylvestris. Journal of Ecology*, 56, 269–307. https://doi.org/10.2307/2258078.

Carvalho, B., Bastias, C.C., Escudero, A., Valladares, F. & Benavides, R. (2020). Intraspecific perspective of plant economics spectrum and phenotypic integration of functional traits in Scots pine. *PLoS ONE* 15(2): e0228539. https://doi.org/10.1371/journal.pone.0228539.

Castro, J., Zamora, R., Hódar, J.A. & Gómez, J.M. (2004). Seedling establishment of a boreal tree species (*Pinus sylvestris*) at its southernmost distribution limit: consequences of being in a marginal Mediterranean habitat. *Journal of Ecology*, 92, 266– 277. https://doi.org/10.1111/j.0022-0477.2004.00870.x.

Chapin, F.S III. (1991). Integrated response of plants to stress. *Bioscience*, 41, 29-36. https://doi.org/10.2307/1311538.

Chave, J., Coomes, D., Jansen, S., Lewis, S.L., Swenson, N.G. & Zanne, A.E. (2009). Towards a worldwide wood economics spectrum. *Ecology Letters*, 12, 351–366. https://doi.org/ 10.1111/j.1461-0248.2009.01285.x.

Cheverud, J.M. (1984). Quantitative genetics and developmental constraints on evolution by selection. *Journal of Theoretical Biology*, 110, 155–171. https://doi.org/10.1016/s0022-5193(84)80050-8.

771 Cheverud, J.M., Wagner, G.P. & Dow, M.M. (1989). Methods for the comparative analysis of
772 variation patterns. *Systematic Zoology*, 38, 201–213. https://doi.org/10.2307/2992282.
773 Conner, J.K. & Hartl, D.L. (2004). A Primer to Ecological Genetics. Sinauer.
774 Csardi, G. & Nepusz, T. (2006). The *igraph* software package for complex network research.
775 *International Journal of Complex Systems*, 1695: http://igraphorg
776 Damián, X., Fornoni, J., Domínguez, C.A. & Boege, K. (2018). Ontogenetic changes in the
777 phenotypic integration and modularity of leaf functional traits. *Functional Ecology*, 32,
778 234-246. https://doi.org/10.1111/1365-2435.12971.
779 Damián, X., Ochoa-López, S., Gaxiola, A., Fornoni, J., Domínguez, C.A. & Boege, K. (2020).
780 Natural selection acting on integrated phenotypes: covariance among functional leaf traits
781 increases plant fitness. *New Phytologist*, 225, 546–557. https://doi.org/10.1111/nph.16116
782 Díaz, S., Kattge, J., Cornelissen, J.H.C., Wright, I.J., Lavorel, S., Dray, S., Reu, B., Kleyer, M.,
783 Wirth, C., Prentice, C., Garnier, E., Bönisch, G., Westoby, M., Poorter, H., Reich, P.B.,
784 Moles, A.T., Dickie, J., Gillison, A.N., Zanne, A.E., Chave, J. et al. (2016). The global
785 spectrum of plant form and function. *Nature*, 529, 167-171.
786 https://doi.org/10.1038/nature16489.
787 Dwyer, J.M. & Laughlin, D.C. (2017a). Constraints on trait combinations explain climatic
788 drivers of biodiversity: the importance of trait covariance in community assembly. *Ecology*
789 *Letters*, 20, 872–882. https://doi.org/10.1111/ele.12781.
790 Dwyer, J.M. & Laughlin, D.C. (2017b). Selection on trait combinations along environmental
791 gradients. *Journal of Vegetation Science*, 28, 672–673. https://doi.org/10.1111/jvs.12567.
792 Fajardo, A. & Piper, F.I. (2011). Intraspecific trait variation and covariation in a widespread
793 tree species (*Nothofagus pumilio*) in southern Chile. *New Phytolo*gist, 189, 259–271.
794 https://doi.org/10.1111/j.1469-8137.2010.03468.x.

795 Fortunel, C. Fine, P.V.A. & Baraloto, C. (2012). Leaf, stem and root tissue strategies across
796 758 Neotropical tree species. *Functional Ecology*, 26, 1153–1161.
797 https://doi.org/10.1111/j.1365-2435.2012.02020.x.
798 Gianoli, E. & Palacio-López, K. (2009). Phenotypic integration may constrain phenotypic
799 plasticity in plants. *Oikos*, 118, 1924-1928. https://doi.org/10.1111/j.1600-
800 0706.2009.17884.x.
801 Gleason, S.M., Westoby, M., Jansen, S., Choat, B., Hacke, U.G., Pratt, R.B., Bhaskar, R.,
802 Brodribb, T.J., Bucci, S.J., Cao, K.F., Cochard, H., Delzon, S., Domec, J.C., Fan, Z-X.,
803 Field, T.S., Jacobsen, A.L., Johnson, D.M., Lens, F., Maherali, H., Martínez-Vilalta, J., et
804 al. (2015). Weak trade-off between xylem safety and xylem- specific hydraulic efficiency
805 across the world's woody plant species. *New Phytologist*, 209, 123–136.
806 https://doi.org/10.1111/nph.13646.
807 Gong, H. & Gao, J. (2019). Soil and climatic drivers of plant SLA (specific leaf area). *Global*
808 *Ecology and Conservation*, 20, e00696. https://doi.org/10.1016/j.gecco.2019.e00696
809 González-Zurdo, P., Escudero, A., Babiano, J., García-Ciudad, A. & Mediavilla, S. (2016)
810 Costs of leaf reinforcement in response to winter cold in evergreen species. *Tree*
811 *Physiology*, 36, 273–286. https://doi.org/10.1093/treephys/tpv134.
812 Grime, J.P. (1977). Evidence for the existence of three primary strategies in plants and its
813 relevance to ecological and evolutionary theory. *The American Naturalist*, 111, 1169-
814 1194. https://doi.org/10.1086/283244
815 Hallgrímsson, B., Jamniczky, H.A., Young, N.M., Rolian, C., Parsons, T.E., Boughner, J.C. &
816 Marcucio, R.S. (2009). Deciphering the palimpsest: studying the relationship between
817 morphological integration and phenotypic covariation. *Evolutionary Biology*, 36, 355–
818 376. https://doi.org/10.1007/s11692-009-9076-5

Holderegger, R., Kamm, U. & Gugerli, F. (2006). Adaptive vs neutral genetic diversity: implications for landscape genetics. *Landscape Ecology*, 21, 797–807. https://doi.org/10.1007/s10980-005-5245-9.

Jernigan, R.W., Culver, D.C. & Fong, D.W. (1994). The dual role of selection and evolutionary history as reflected in genetic correlations. *Evolution*, 48, 587–596. https://doi.org/10.1111/j.1558-5646.1994.tb01346.x.

Jung, V., Albert, C.H., Violle, C., Kunstler, G., Loucougaray, G. & Spiegelberger, T. (2014). Intraspecific trait variability mediates the response of subalpine grassland communities to extreme drought events. *Journal of Ecology*, 102, 45-53. https://doi.org/10.1111/1365-2745.12177.

Karger, D.N., Conrad, O., Böhner, J., Kawohl, T., Kreft, H., Soria-Auza, R.W., Zimmermann, N.E., Linder, H.E. & Michael Kessler. (2017a). Climatologies at high resolution for the earth's land surface areas. *Scientific Data*, 4, 170122. https://doi.org/10.1038/sdata.2017.122.

Karger, D.N., Conrad, O., Böhner, J., Kawohl, T., Kreft, H., Soria-Auza, R.W., Zimmermann, N.E., Linder, H.E. & Michael Kessler. (2017b). Data from: Climatologies at high resolution for the earth's land surface areas. *Dryad Digital Repository*. https://doi.org/105061/dryadkd1d4.

Kawecki, T.J. & Ebert, D. (2004). Conceptual issues in local adaptation. *Ecology Letters*, 7, 1225–1241. https://doi.org/10.1111/j.1461-0248.2004.00684.x.

Kirkpatrick, M. & Barton, N.H. (1997). Evolution of a species' range. *The American Naturalist*, 150: 1-23. https://doi.org/10.1086/286054

Klingenberg, C.P. (2014). Studying morphological integration and modularity at multiple levels: concepts and analysis. *Philosophical Transactions of the Royal Society B.*, 369, 20130249. https://doi.org/10.1098/rstb.2013.0249

844 Kraft, N.J.B., Godoy, O. & Levine, J.M. (2015). Plant functional traits and the
845 multidimensional nature of species coexistence. *Proceedings of the National Academy of*
846 *Sciences, USA*, 112, 797-802. https://doi.org/10.1073/pnas.1413650112
847 Laforest-Lapointe, I., Martínez-Vilalta, J. & Retana, J. (2014). Intraspecific variability in
848 functional traits matters: case study of Scots pine. *Oecologia*, 175, 1337–1348.
849 https://doi.org/10.1007/s00442-014-2967-x.
850 Leimu, R. & Fischer, M. (2008). A meta-analysis of local adaptation in plants. *PLoS ONE* 3,
851 e4010. https://doi.org/10.1371/journal.pone.0004010
852 Lorimer, C.G. (1983). Tests of age-independent competition indices for individual trees in
853 natural hardwood stands. *Forest Ecology and Manage*ment, 6, 343-360.
854 https://doi.org/10.1016/0378-1127(83)90042-7.
855 Lotterhos, K.E. & Whitlock, M.C. (2015). The relative power of genome scans to detect local
856 adaptation depends on sampling design and statistical method. *Molecular Ecology*, 24,
857 1031-1046. https://doi.org/10.1111/mec.13100.
858 Luo, Y. Hu, H., Zhao, M., Li, H., Liu, S. & Fang, J. (2019). Latitudinal pattern and the driving
859 factors of leaf functional traits in 185 shrub species across eastern China. *Journal of Plant*
860 *Ecology*, 12, 67–77. https://doi.org/10.1093/jpe/rtx065.
861 Lusk, C.H., Reich, P.B., Montgomery, R.A., Ackerly, D.D. & Cavender-Bares, J. (2008) Why
862 are evergreen leaves so contrary about shade? *Trends in Ecology & Evolution*, 23, 299–
863 303. https://doi.org/10.1016/j.tree.2008.02.006
864 Maire, V., Gross, N., Hill, D., Martin, R., Wirth, C., Wright, I.J. & Soussana, J.F. (2013).
865 Disentangling coordination among functional traits using an individual-centred model:
866 impact on plant performance at intra- and inter-specific levels. *PLoS ONE*, 8, e77372.
867 https://doi.org/10.1371/journal.pone.0077372.
868 Martin, A.R., Rapidel, B., Roupsard, O., Van den Meersche, K., de Melo Virginio Filho, E.,
869 Barrios, M. & Isaac, M.E. (2017). Intraspecific trait variation across multiple scales: the

leaf economics spectrum in coffee. *Functional Ecology*, 31, 604–612. https://doi.org/10.1111/1365-2435.12790.

Martínez-Sancho, E., Slámová, L., Morganti, S., Grefen, C., Carvalho, B., Dauphin, B., Rellstab, C., Gugerli, F., Opgenoorth, L., Heer, K., Knutzen, F., von Arx, G., Valladares, F., Cavers, S., Fady, B., Alía, R., Aravanopoulos, F., Avanzi, C., Bagnoli, F., Barbas, E. et al. (2019). The GenTree Dendroecological Collection, tree-ring and wood density data from seven tree species across Europe. *figshare.* https://doi.org/10.6084/m9.figshare.c.4561037.

Martínez-Sancho, E., Slámová, L., Morganti, S., Grefen, C., Carvalho, B., Dauphin, B., Rellstab, C., Gugerli, F., Opgenoorth, L., Heer, K., Knutzen, F., von Arx, G., Valladares, F., Cavers, S., Fady, B., Alía, R., Aravanopoulos, F., Avanzi, C., Bagnoli, F., Barbas, E. et al. (2020). The GenTree Dendroecological Collection, tree-ring and wood density data from seven tree species across Europe. *Scientific Data*, 7, 1. https://doi.org/10.1038/s41597-019-0340-y.

Mauri, A., Strona, G. & San-Miguel-Arranz, J. (2017). Data Descriptor: EU-Forest, a high-resolution tree occurrence dataset for Europe. *Scientific Data*, 4, 160123. https://doi.org/10.1038/sdata.2016.123.

Merilä, J. & Björklund, M. (2004). Phenotypic integration as a constraint and adaptation. In M. Pigliucci & K. Preston (Eds) *Phenotypic Integration: studying the ecology and evolution of complex phenotypes* (pp. 107-129). Oxford University Press.

Messier, J., McGill, B.J., Enquist, B.J. & Lechowicz, M.J. (2017). Trait variation and integration across scales: is the leaf economic spectrum present at local scales? *Ecography*, 40, 685-697. https://doi.org/10.1111/ecog.02006.

Messier, J., Violle, C., Enquist, B.J., Lechowicz, M.J. & McGill, B.J. (2018). Similarities and differences in intrapopulation trait correlations of co-occurring tree species: consistent

895 water-use relationships amid widely different correlation patterns. *American Journal of*
896 *Botany*, 105, 1477–1490. https://doi.org/10.1002/ajb2.1146.
897 Michelaki, C., Fyllas, N.M., Galanidis, A., Aloupi, M., Evangelou, E., Arianoutsou, M.,
898 Dimitrakopoulos, P.G. (2019). An integrated phenotypic trait-network in thermo-
899 Mediterranean vegetation describing alternative, coexisting resource-use strategies.
900 *Science of the Total Environment*, 672, 583–592.
901 https://doi.org/10.1016/j.scitotenv.2019.04.030.
902 Murren, C.J. (2002). Phenotypic integration in plants. *Plant Species Biology*, 17, 89-99.
903 https://doi.org/10.1046/j.1442-1984.2002.00079.x.
904 Nicotra, A.B., Chazdon, R.L. & Schlichting, C.D. (1997). Patterns of genotypic variation and
905 phenotypic plasticity of light response in too tropical *Piper* (Piperaceae) species. *American*
906 *Journal of Botany*, 84, 1542-1552. https://doi.org/10.2307/2446616.
907 Niklas, K.J. (1999). The mechanical role of bark. *American Journal of Botany*, 86, 465-469.
908 https://doi.org/10.2307/2656806.
909 Olson, E.C. & Miller, R.J. 1958. Morphological integration. University of Chicago Press.
910 Opgenoorth, L., Dauphin, B., Benavides, R., Heer, K., Alizoti, P., Martínez-Sancho, E., Alía,
911 R., Ambrosio, O., Albet, A., Aravanopoulos, F., Auñón, F., Avanzi, C., Avramidou, E.,
912 Bagnoli, F., Ballesteros, E., Barbas, E., Bastias, C.C., Bastien, C., Bernier, F., Bignalet, H.
913 et al.,.(2021) The GenTree Platform: growth traits and tree-level environmental data in
914 twelve European forest tree species. *GigaScience* 10, 1–13.
915 https://doi:10.1093/gigascience/giab010
916 Opgenoorth, L., Dauphin, B., Benavides, R., Heer, K., Alizoti, P., Martínez-Sancho, E., Alía,
917 R., Ambrosio, O., Albet, A., Aravanopoulos, F., Auñón, F., Avanzi, C., Avramidou, E.,
918 Bagnoli, F., Ballesteros, E., Barbas, E., Bastias, C.C., Bastien, C., Bernier, F., Bignalet, H.
919 et al., (2020). The GenTree-Platform. *figshare*
920 https://figshare.com/s/4d57474fd63864a6dfd8.

921 Paine, C.E.T., Stahl, C., Courtois, E.A., Sarmiento, C. & Baraloto, C. (2010). Functional
922 explanations for variation in bark thickness in tropical rain forest trees. *Functional*
923 *Ecology*, 24, 1202-1210. https://doi.org/10.1111/j.1365-2435.2010.01736.x.
924 Pereira, J.S. & Chaves, M.M. (1995). Plant Responses to Drought Under Climate Change in
925 Mediterranean-Type Ecosystems. In J.M. Moreno & W.C Oechel (Eds) *Global Change*
926 *and Mediterranean-Type Ecosystems*. Ecological Studies (Analysis and Synthesis), vol
927 117 Springer.
928 Pérez-Harguindeguy, N., Díaz, S., Garnier, E., Lavorel, S., Poorter, H., Jaureguiberry, P., Bret-
929 Harte, M. S. ., Cornwell, W. K., Craine, J. M., Gurvich, D. E., Urcelay, C., Veneklaas, E.
930 J., Reich, P. B., Poorter, L., Wright, I. J., Ray, P., Enrico, L., Pausas, J. G., de Vos, A. C.,
931 Buchmann, N. et al. (2013). New handbook for standardised measurement of plant
932 functional traits worldwide. *Australian Journal of Botany*, 61, 167-234.
933 https://doi.org/10.1071/BT12225.
934 Pigliucci, M. (2001). *Phenotypic plasticity: beyond nature and nurture*. Baltimore, USA: Johns
935 Hopkins University Press.
936 Pigliucci, M. (2003). Phenotypic integration: studying the ecology and evolution of complex
937 phenotypes. *Ecology Letters*, 6, 265–272. https://doi.org/10.1046/j.1461-
938 0248.2003.00428.x.
939 Pigliucci, M. (2004). Studying the plasticity of phenotypic integration in a model organism. In
940 M. Pigliucci & K. Preston (Eds) *Phenotypic Integration: studying the ecology and*
941 *evolution of complex phenotypes* (pp. 155-175). Oxford University Press.
942 Pigliucci, M. & Kolodynska, A. (2002a). Phenotypic plasticity and integration in response to
943 flooded conditions in natural accessions of *Arabidopsis thaliana* (L) Heynh
944 (Brassicaceae). *Annals of Botany*, 90, 199-207. https://doi.org/10.1093/aob/mcf164.

945 Pigliucci, M. & Kolodynska, A. (2002b). Phenotypic plasticity to light intensity in *Arabidopsis*
946 *thaliana*: invariance of reaction norms and phenotypic integration. *Evolutionary Ecology*,
947 16, 27-47. https://doi.org/10.1023/A:1016073525567.
948 Pigliucci, M. & Kolodynska, A. (2006). Phenotypic integration and response to stress in
949 *Arabidopsis thaliana*: a path analytical approach. *Evolutionary Ecology Research*, 8, 415-
950 433.
951 Pyhäjärvi, T., Kujala, S.T. & Savolainen, O. (2019). 275 years of forestry meets genomics in
952 *Pinus sylvestris*. *Evolutionary applications*, 13, 11–30. https://doi.org/10.1111/eva.12809.
953 R Core Team. (2019). R: A language and environment for statistical computing. Foundation
954 for Statistical Computing. https://wwwR-projectorg/
955 Reich, P.B. (2014). The world-wide 'fast-slow' plant economics spectrum: a traits manifesto.
956 *Journal of Ecology*, 102, 275–301. https://doi.org/10.1111/1365-2745.12211.
957 Robledo-Arnuncio, J.J., Smouse, P.E., Gil, L. & Alía, R. (2004). Pollen movement under
958 alternative silvicultural practices in native populations of Scots pine *(Pinus sylvestris* L)
959 in central Spain. *Forest Ecology and Management*, 197, 245–255.
960 https://doi.org/10.1016/j.foreco.2004.05.016.
961 Rosas, T., Mencuccini, M., Barba, J., Cochard, H., Saura-Mas, S., Martínez-Vilalta, J. (2019).
962 Adjustments and coordination of hydraulic leaf and stem traits along a water availability
963 gradient. *New Phytologist*, 223, 632–646. https://doi.org/10.1111/nph.15684.
964 Sexton, J.P., McIntyre, P.J., Angert, A.L. & Rice, K.J. (2009). Evolution and Ecology of
965 Species Range Limits. *Annual Review of Ecology Evolution and Systematics*, 40, 415–436.
966 https://doi.org/10.1146/annurev.ecolsys.110308.120317
967 Schlichting, C.D. (1986). The evolution of phenotypic plasticity in plants. *Annual Review of*
968 *Ecology and Systematics*, 17, 667-693.
969 https://doi.org/10.1146/annurev.es.17.110186.003315.

970 Schlichting, C.D. (1989). Phenotypic plasticity in Phlox: II Plasticity of character correlations.
971 *Oecologia*, 78, 496–501. https://doi.org/10.1007/BF00378740.
972 Soule, M. (1973). The epistasis cycle: a theory of marginal populations. *Annual Review of*
973 *Ecology, Evolution, and Systematics*, 165–187.
974 https://doi.org/10.1146/annurev.es.04.110173.001121
975 Stamp, M.A. & Hadfield, J.D. (2020). The relative importance of plasticity versus genetic
976 differentiation in explaining between population differences; a meta-analysis. *Ecology*
977 *Letters*, 23, 1432-1441. https://doi.org/101111/ele13565.
978 Umaña, M.N. & Swenson, N.G. (2019). Does trait variation within broadly distributed species
979 mirror patterns across species? A case study in Puerto Rico. *Ecology*, 100, e02745.
980 https://doi.org/10.1002/ecy.2745.
981 Valladares, F., Gianoli, E. & Gómez, J.M. (2007). Ecological limits to plant phenotypic
982 plasticity. *New Phytologist*, 176, 749–763. https://doi.org/10.1111/j.1469-
983 8137.2007.02275.x.
984 Wachowiak, W., Wójkiewicz, B., Cavers, S. & Lewandowski, A. (2014). High genetic
985 similarity between Polish and North European Scots pine (*Pinus sylvestris* L) populations
986 at nuclear gene loci. *Tree Genetics & Genomes*, 10, 1015–1025.
987 https://doi.org/10.1007/s11295-014-0739-8.
988 Wagner, G.P. (1984). On the eigenvalue distribution of genetic and phenotypic dispersion
989 matrices: Evidence for a non-random organization of quantitative character variation.
990 *Journal of Mathematical Biology*, 21, 77-95. https://doi.org/10.1007/BF00275224
991 Wagner, G.P., Pavlicev, M. & Cheverud J. (2007). The road to modularity. *Nature Genetics*,
992 8, 921-931. https://doi.org/ 10.1038/nrg2267.
993 Westoby, M. (1998). A leaf-height-seed (LHS) plant ecology strategy scheme. *Plant and Soil*,
994 199, 213-227. https://doi.org/ 10.1023/A:1004327224729.

995 Westoby, M., Falster, D.S., Moles, A.T., Vesk, P.A., Wright, I.J. (2002). Plant ecological
996 strategies: some leading dimensions of variation between species. *Annual Review of*
997 *Ecology, Evolution, and Systematics*, 33, 125–59.
998 https://doi.org/10.1146/annurev.ecolsys.33.010802.150452.
999 Westoby, M., Leishman, M.R. & Lord, J.M. 1995. On misinterpreting the "phylogenetic
1000 correction". *Journal of Ecology*, 83, 531-534. https://doi.org/ 10.2307/2261605.
1001 Westoby, M. & Wright, I.J. 2006. Land-plant ecology on the basis of functional traits. *Trends*
1002 *in Ecology & Evolution*, 21, 261–268. https://doi.org/10.1016/j.tree.2006.02.004.
1003 Wilson, P.J., Thompson, K. & Hodgson, J.G. (1999). Specific leaf area and leaf dry matter 1004
content as alternative predictors of plant strategies. *New Phytologist*, 143, 155–162.
1005 https://doi.org/ 10.1046/j.1469-8137.1999.00427.x.
1006 Wickham, H. (2016). ggplot2: Elegant Graphics for Data Analysis. Springer-Verlag.
1007 Wright, I.J., Dong, N., Maire, V., Prentice, C., Westoby, M., Díaz, S., Gallagher, R.R., Jacobs,
1008 B.F., Kooyman, R., Law, E.A., Leishman, M.R., Niinemets, Ü., Reich, P.B., Sack, L., 1009
Villar, R., Wang, H. & Wilf, P. (2017). Global climatic drivers of leaf size. *Science*, 357,
1010 917–921. https://doi.org/10.1126/science.aal4760
1011 Wright, I.J., Reich, P.B., Westoby, M., Ackerly, D.D., Baruch, Z., Bongers, F., Cavender- 1012
Bares, J., Chapin, T., Cornelissen, J.H.C., Diemer, M., Flexas, J., Garnier, E., Groom, P.K.,
1013 Gulias, J., Hikosaka, K., Lamont, B.B., Lee, T., Lee, W., Lusk, C., Midgley, J.J. et al. 1014
(2004). The worldwide leaf economics spectrum. *Nature*, 428, 821-827.
1015 https://doi.org/10.1038/nature02403.
1016 Zeileis, A. & Hothorn, T. (2002). Diagnostic Checking in Regression Relationships. *R News*,
1017 2(3), 7-10. https://CRAN.R-project.org/doc/Rnews/
1018 Zuur, A.F., Ieno, E.N., Walker, N.J., Saveliev, A.A. & Smith, G.M. (2009). Mixed effects
1019 models and extensions in ecology with R. Springer-Verlag.

Appendix A. Information about the study sites

Table S1. **Description of the study sites.** Headings are: Country; Local gradient; Class - classification within the local gradient: mild (M) or harsh (H) conditions, or unpaired (UNP); PopID - population code; Lat - latitude; Long - longitude; Elevation (m); Age – average population age (yrs); T - mean annual temperature (ºC); P - mean annual precipitation (mm); $BAI_{2006-2015}$ - mean basal area increment (cm^2); BAI_{st} - mean basal area increment standardised by age, size and competition index; and two metrics of trait covariation: ED - edge density (%) and FS - functional variability shape, estimated as variance of the eigenvalues of the correlation matrices. Sites are ordered by latitude, showing first the population in mild conditions (M).

Country	Local gradient	Class	PopID	Lat	Long	Elevation	Age	T	P	$BAI_{2006-2015}$	BAI_{st}	ED	FS
Greece	elevation	M	GR_10	40.27	22.208	1698.4	114	6.2	638	377.51	0.0146	27.8	0.94
		H	GR_09	40.193	22.143	1268.8	40	8.3	566	427.14	-0.0146	30.6	1.26
Spain	elevation	M	ES_02	40.996	-3.822	1836.2	86.5	6.9	719	136.79	0.1054	17.8	0.64
		H	ES_01	41.028	-3.81	1458	100.1	9	641	136.59	0.097	24.4	0.62
Italy	elevation	M	IT_08	44.537	10.54	713.2	83.2	10.9	911	64.62	0.0613	20	0.80
		H	IT_07	44.536	10.524	420.2	62.6	12	775	84.79	-0.0613	31.1	0.82
France	elevation	M	FR_04	45.403	3.695	759.3	111.8	9.5	678	138.34	0.0236	22.2	0.62
		H	FR_03	45.568	3.931	1251.3	64.4	6.5	973	214.94	-0.0236	26.7	0.78
Switzerland	elevation	M	CH_06	46.093	7.074	538.4	109.9	9.9	659	151.74	0.0493	26.7	0.80
		H	CH_05	46.133	7.074	1193.3	123	7.6	937	102.23	-0.0493	42	1.18
Germany	soil type, continentaly	M	DE_12	52.975	13.666	80	126.7	8.9	585	213.89	0.1478	22.2	0.85
		H	DE_11	53.263	13.138	82.8	108	8.8	576	118.79	-0.1421	28.9	0.80
Lithuania	–	Unp	LT_20	54.025	24.438	144.8	110.1	7	649	112.59	-	28.9	1.00
G. Britain	water availability elevation	M	GB_14	57.208	-3.614	359	125.1	6.9	747	234.28	0.0565	22.2	0.79
		H	GB_13	57.63	-5.354	57.4	176	8.7	1427	171.76	-0.052	30.6	0.93
Norway	elevation	M	NO_15	59.868	11.055	304.9	158	4.9	953	88.72	0.0665	26.7	0.88
		H	NO_16	61.458	12.421	701.7	137.5	1.8	750	69.77	-0.0665	28.9	1.00
Sweden	–	Unp	SE_17	63.963	20.351	94.8	65.9	3.1	690	67.10	-	31.1	0.82
Finland	day-length	M	FI_19	61.656	29.291	87.2	95.9	3.8	597	138.55	0.0739	22.2	0.87
		H	FI_18	66.439	26.785	192	75.6	0.6	541	40.57	-0.0739	63.9	2.20

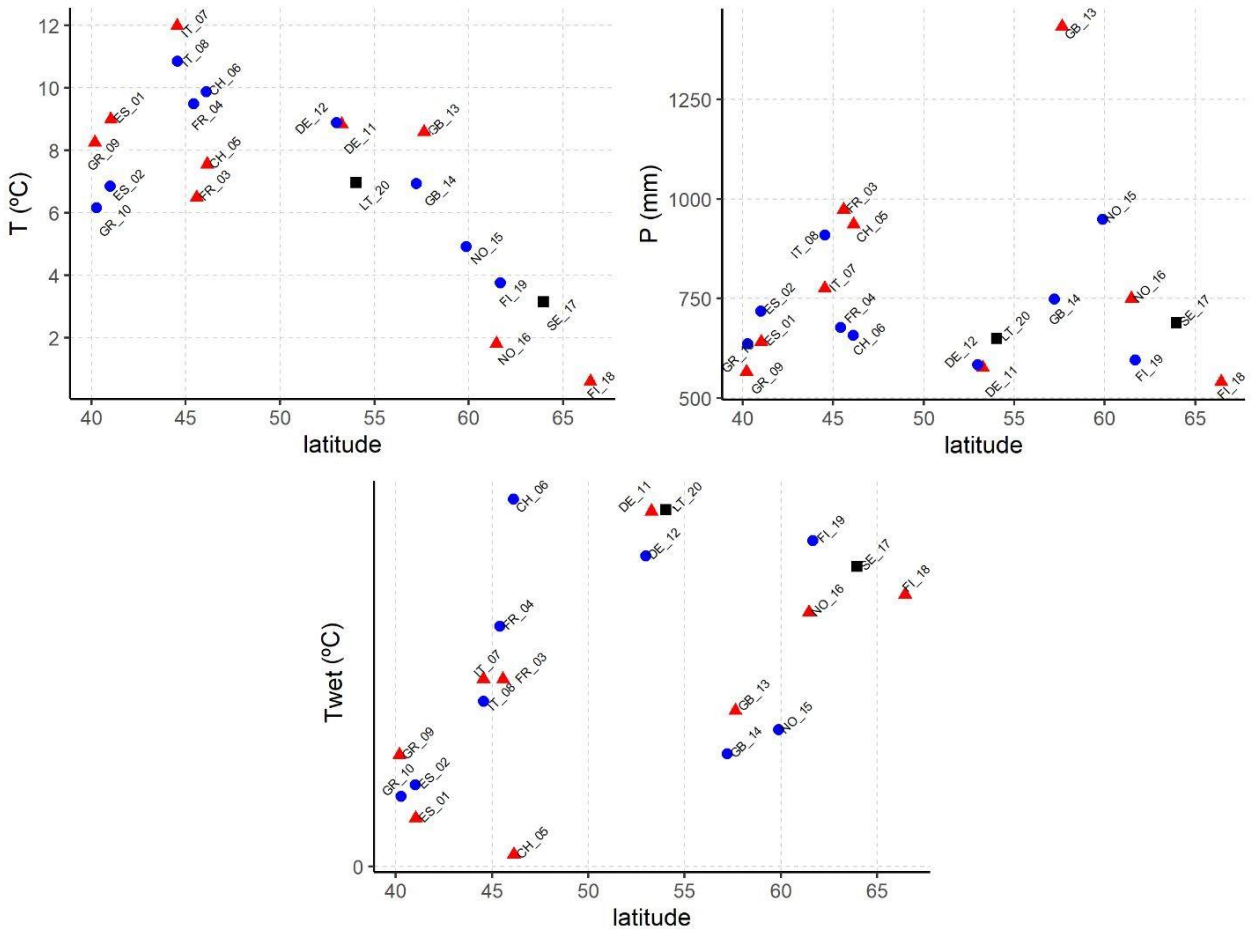

Fig. S1. Variation in mean annual temperature (T), precipitation (P) and mean temperature of the wettest quarter (Twet) of the study populations across latitude. Climatic variables were obtained from CHELSA (http://chelsa-climate.org/). Populations are labelled with their site code based on their country location (ES: Spain, GR: Greece, IT: Italy, FR: France, CH: Switzerland, DE: Germany, GB: Great Britain, LT: Lithuania, NO: Norway, SE: Sweden, FI: Finland) and a number between 1 and 20. Red triangles represent the populations within a pair that were classed as occupying harsher conditions; blue circles represent the populations within a pair that were classed as occupying milder conditions, and black squares represent unpaired locations.

Selection of environmental variables that capture the environmental variability of the study sites.

We used environmental data for the study sites compiled in Opgenoorth et al. (2020), which in turn were retrieved from CHELSA (c.a. 1 km^2) (Karger et al., 2017a, b). Selections among the 26 climatic variables were made based on a Principal Component Analysis, looking for those that captured more variance within the first three dimensions and checking that the selected variables were not strongly correlated ($\rho<0.4$, see Table S2). Based on these criteria, and favouring more common variables, we finally selected mean annual temperature (bio01), annual precipitation sum (bio12) and temperature of the wettest quarter of the year (bio08). PCA was implemented using *prcomp* function from *stats* package R (R Core Team, 2019) and *fviz_pca_var* function from *factoextra* R package (Kassambara & Mundt, 2020).

The 26 variables were: mean annual temperature (bio01), mean diurnal range (bio02), isothermality (bio03), temperature seasonality (bio04), max temperature of warmest month (bio05), min temperature of coldest month (bio06) temperature annual range (bio07), mean temperature of wettest quarter (bio08), mean temperature of driest quarter (bio09), mean temperature of warmest quarter (bio10), mean temperature of coldest quarter (bio11), annual precipitation sum (bio12), precipitation of wettest month (bio13), precipitation of driest month (bio14), precipitation seasonality (bio15), precipitation of wettest quarter (bio16), precipitation of driest quarter (bio17), precipitation of warmest quarter (bio18), precipitation of coldest quarter (bio19), growing degree days (ggd), accumulated precipitation (gsp), relative humidity (rh410, between April and October), frost change frequency (fcf), number of frost days (nfd), potential evapotranspiration between April and October (PET410), moisture deficit, assessed as PET-bio12 (MD).

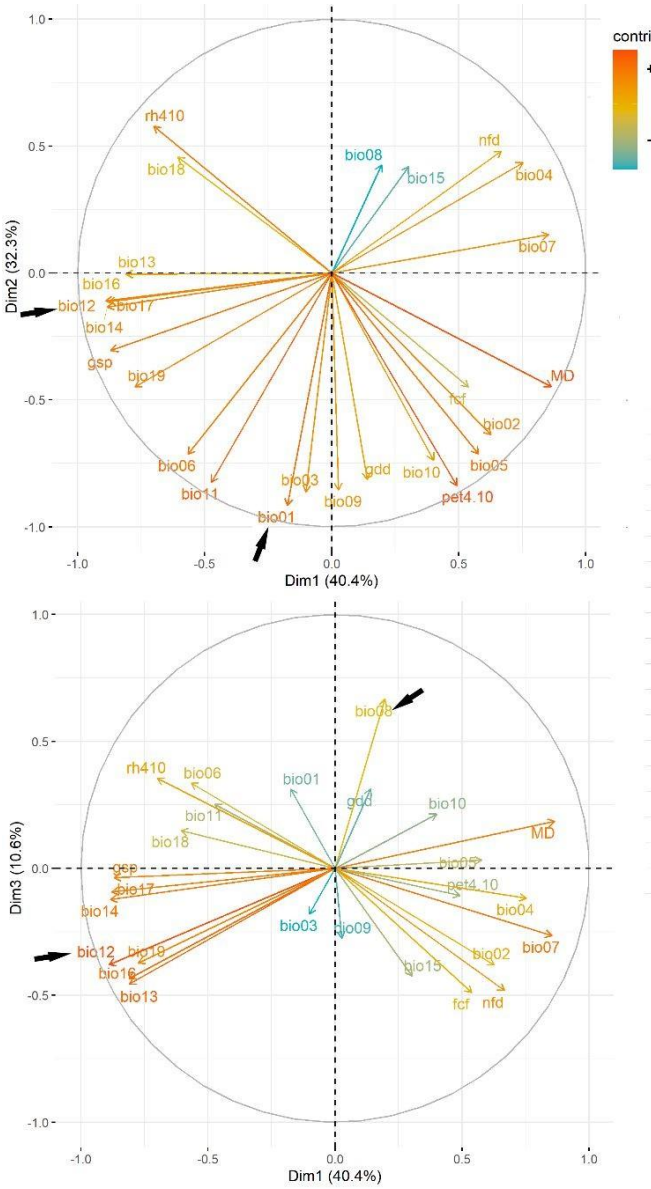

	PC1	PC2	PC3
bio01	-0.04	**-0.32**	0.17
bio02	0.20	-0.21	-0.23
bio03	-0.02	-0.30	-0.10
bio04	0.23	0.16	-0.08
bio05	0.18	-0.24	0.00
bio06	-0.17	-0.26	0.20
bio07	0.26	0.06	-0.17
bio08	0.05	0.14	**0.39**
bio09	0.02	-0.29	-0.16
bio10	0.13	-0.25	0.11
bio11	-0.14	-0.29	0.15
bio12	**-0.27**	-0.05	-0.24
bio13	-0.25	-0.01	-0.29
bio14	-0.27	-0.05	-0.07
bio15	0.09	0.15	-0.28
bio16	-0.25	-0.01	-0.28
bio17	-0.27	-0.05	-0.05
bio18	-0.20	0.14	0.07
bio19	-0.23	-0.16	-0.22
gdd	0.05	-0.28	0.17
gsp	-0.26	-0.12	-0.04
rh410	-0.23	0.19	0.21
fcf	0.17	-0.14	-0.29
nfd	0.20	0.18	-0.29
pet410	0.16	-0.28	-0.07
MD	0.27	-0.15	0.11

Fig. S2. **PCA biplots (left) and loadings (right) based on analysis of data for 26 climatic variables from each population**. Black arrows indicate variables selected as representative of most variation in the dataset.

Similarly, we gathered 16 topographic variables derived from the European digital elevation model with 25m spatial resolution (EU-DEM v.1.1, Copernicus program; https://land.copernicus.eu/), and available water capacity data using SoilGrids250m, from Opgenoorth et al. (2020). The variables included were: altitude (t01alt), slope (t02slp), eastness (t03asp), profile curvature

(t04vcu), horizontal curvature (t05hcu), downslope distance gradient (t06ddg), morphometric protection index (t07mpi), topographic position index (t08tpi), vector ruggedness measure (t09vrm), topographic wetness index (t10twi), sky-view factor (t11svf), potential direct solar radiation (t12sdir), potential diffuse solar radiation (t13sdif), potential total solar radiation (t14stot), available water capacity (0-30cm), and available water capacity (60-200cm).

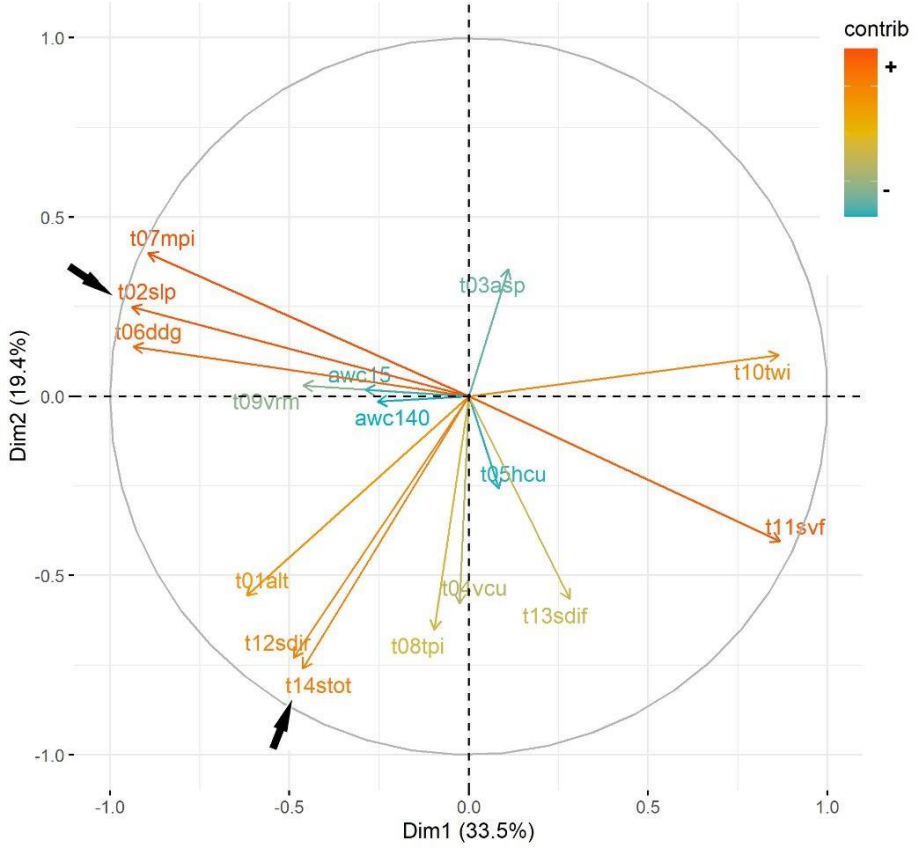

	PC1	PC2
t01alt	-0.27	-0.32
t02slp	**-0.41**	0.14
t03asp	0.05	0.20
t04vcu	-0.01	-0.33
t05hcu	0.04	-0.15
t06ddg	-0.40	0.08
t07mpi	-0.39	0.23
t08tpi	-0.04	-0.37
t09vrm	-0.20	0.02
t10twi	0.37	0.07
t11svf	0.38	-0.23
t12sdir	-0.21	-0.41
t13sdif	0.12	-0.32
t14stot	-0.20	**-0.43**
awc15	-0.12	0.01
awc140	-0.11	-0.01

Fig. S3. **PCA biplot (left) and loadings (right) based on analysis of data for 16 topographic variables from each population**. Black arrows indicate variables selected as representative of most variation in the dataset.

Table S2. Spearman correlation coefficients among climatic variables in the study sites. Data extracted from CHELSA (Karger et al., 2017a, b), and compiled in Opgenoorth et al. (2020)

	bio01	bio02	bio03	bio04	bio05	bio06	bio07	bio08	bio09	bio10	bio11	bio12	bio13	bio14	bio15	bio16	bio17	bio18	bio19	gdd	gsp	rh410	fcf	nfd	pet4.10	MD
bio01	1.00	0.40	0.42	-0.49	0.74	0.78	-0.33	-0.01	0.71	0.81	0.84	0.06	-0.14	0.23	-0.49	-0.20	0.20	-0.25	0.35	0.92	0.58	-0.46	0.19	-0.82	0.66	0.30
bio02		1.00	0.73	-0.07	0.81	-0.01	0.29	-0.47	0.65	0.64	0.13	-0.05	0.04	-0.26	-0.01	-0.03	-0.30	-0.48	0.26	0.53	-0.04	-0.89	0.82	0.04	0.92	0.77
bio03			1.00	-0.66	0.47	0.41	-0.25	-0.64	0.69	0.33	0.47	0.17	0.03	0.01	-0.28	-0.06	-0.02	-0.36	0.61	0.35	0.19	-0.57	0.72	-0.30	0.68	0.31
bio04				1.00	-0.02	-0.83	0.83	0.36	-0.46	-0.02	-0.77	-0.40	-0.06	-0.39	0.49	0.02	-0.38	0.01	-0.68	-0.22	-0.55	0.01	-0.19	0.71	0.07	0.40
bio05					1.00	0.23	0.26	-0.06	0.65	0.96	0.35	-0.22	-0.18	-0.23	-0.11	-0.24	-0.27	-0.52	0.06	0.88	0.14	-0.82	0.52	-0.27	0.93	0.79
bio06						1.00	-0.72	-0.11	0.56	0.31	0.97	0.27	-0.05	0.42	-0.56	-0.10	0.41	-0.08	0.52	0.53	0.67	-0.02	-0.07	-0.96	0.26	-0.10
bio07							1.00	0.02	-0.07	0.18	-0.59	-0.42	-0.04	-0.55	0.59	0.01	-0.57	-0.32	-0.46	-0.06	-0.57	-0.30	0.03	0.63	0.38	0.59
bio08								1.00	-0.55	0.09	-0.21	-0.35	-0.39	-0.08	-0.01	-0.34	-0.06	0.15	-0.66	0.10	-0.06	0.40	-0.41	0.06	-0.27	0.06
bio09									1.00	0.57	0.70	0.18	0.12	0.09	-0.20	0.07	0.04	-0.46	0.64	0.62	0.30	-0.68	0.43	-0.54	0.69	0.35
bio10										1.00	0.40	-0.25	-0.26	-0.13	-0.22	-0.31	-0.16	-0.46	0.00	0.94	0.22	-0.73	0.38	-0.38	0.84	0.67
bio11											1.00	0.31	0.01	0.41	-0.52	-0.04	0.40	-0.12	0.61	0.59	0.68	-0.15	-0.04	-0.95	0.41	0.01
bio12												1.00	0.86	0.80	-0.36	0.83	0.80	0.64	0.78	-0.13	0.73	0.18	-0.07	-0.25	-0.27	-0.81
bio13													1.00	0.54	0.05	0.98	0.54	0.57	0.57	-0.20	0.51	0.09	-0.05	0.04	-0.32	-0.82
bio14														1.00	-0.70	0.55	1.00	0.70	0.64	0.06	0.81	0.30	-0.14	-0.44	-0.25	-0.73
bio15															1.00	0.05	-0.69	-0.24	-0.45	-0.36	-0.60	0.00	-0.17	0.56	-0.20	-0.03
bio16																1.00	0.55	0.60	0.54	-0.26	0.48	0.16	-0.11	0.07	-0.32	-0.82
bio17																	1.00	0.73	0.62	0.03	0.81	0.35	-0.19	-0.43	-0.27	-0.73
bio18																		1.00	0.20	-0.34	0.51	0.64	-0.37	0.03	-0.58	-0.72
bio19																			1.00	0.12	0.63	-0.18	0.24	-0.46	0.01	-0.53
gdd																				1.00	0.40	-0.61	0.33	-0.59	0.76	0.50
gsp																					1.00	0.13	-0.14	-0.71	-0.13	-0.65
rh410																						1.00	-0.75	0.01	-0.86	-0.77
fcf																							1.00	0.17	0.73	0.60
nfd																								1.00	0.02	0.26
pet4.10																									1.00	0.78
MD																										1.00

mean annual temperature (bio01), mean diurnal range (bio02), isothermality (bio03), temperature seasonality (bio04), max temperature of warmest month (bio05), min temperature of coldest month (bio06) temperature annual range (bio07), mean temperature of wettest quarter (bio08), mean temperature of driest quarter (bio09), mean temperature of warmest quarter (bio10), mean temperature of coldest quarter (bio11), annual precipitation sum (bio12), precipitation of wettest month (bio13), precipitation of driest month (bio14), precipitation seasonality (bio15), precipitation of wettest quarter (bio16), precipitation of driest quarter (bio17), precipitation of warmest quarter (bio18), precipitation of coldest quarter (bio19), growing degree days (ggd), accumulated precipitation (gsp), relative humidity between April and October (rh410), frost change frequency (fcf), number of frost days (nfd), potential evapotranspiration between April and October (PET410), moisture deficit = PET-bio12 (MD).

Table S3. Spearman correlation coefficients among topographic variables. Variables derived from the European digital elevation model (EU-DEM v.1.1 Copernicus program; http://land.copernicus.eu/) and compiled in Opgenoorth et al. (2020).

	t01alt	t02slp	t03asp	t04vcu	t05hcu	t06ddg	t07mpi	t08tpi	t09vrm	t10twi	t11svf	t12sdir	t13sdif	t14stot	awc15	awc140
t01alt	1.00	0.57	-0.14	0.12	0.05	0.59	0.50	0.18	0.47	-0.58	-0.52	0.65	0.48	0.66	0.46	0.43
t02slp		1.00	-0.07	-0.01	-0.02	0.89	0.95	0.04	0.67	-0.92	-0.97	0.40	-0.21	0.38	0.45	0.35
t03asp			1.00	-0.02	-0.03	-0.12	-0.06	-0.02	-0.20	0.14	0.11	-0.23	-0.22	-0.24	-0.06	-0.06
t04vcu				1.00	0.32	0.06	-0.20	0.80	0.23	-0.06	0.06	0.25	0.02	0.25	-0.04	-0.07
t05hcu					1.00	-0.02	-0.20	0.58	0.24	-0.16	0.07	0.16	-0.07	0.16	-0.10	-0.14
t06ddg						1.00	0.86	0.11	0.68	-0.85	-0.90	0.38	-0.16	0.36	0.42	0.33
t07mpi							1.00	-0.18	0.57	-0.84	-0.97	0.31	-0.21	0.30	0.48	0.40
t08tpi								1.00	0.31	-0.19	0.03	0.34	0.00	0.34	-0.06	-0.10
t09vrm									1.00	-0.75	-0.68	0.48	-0.19	0.46	0.32	0.22
t10twi										1.00	0.89	-0.45	0.15	-0.43	-0.44	-0.34
t11svf											1.00	-0.37	0.25	-0.35	-0.49	-0.39
t12sdir												1.00	0.10	1.00	0.03	-0.02
t13sdif													1.00	0.15	0.31	0.43
t14stot														1.00	0.04	0.00
awc15															1.00	0.97
awc140																1.00

altitude (t01alt), slope (t02slp), eastness (t03asp), profile curvature (t04vcu), horizontal curvature (t05hcu), downslope distance gradient (t06ddg), morphometric protection index (t07mpi), topographic position index (t08tpi), vector ruggedness measure (t09vrm), topographic wetness index (t10twi), sky-view factor (t11svf), potential direct solar radiation (t12sdir), potential diffuse solar radiation (t13sdif), potential total solar radiation (t14stot), available water capacity (0-30cm), and available water capacity (60-200cm).

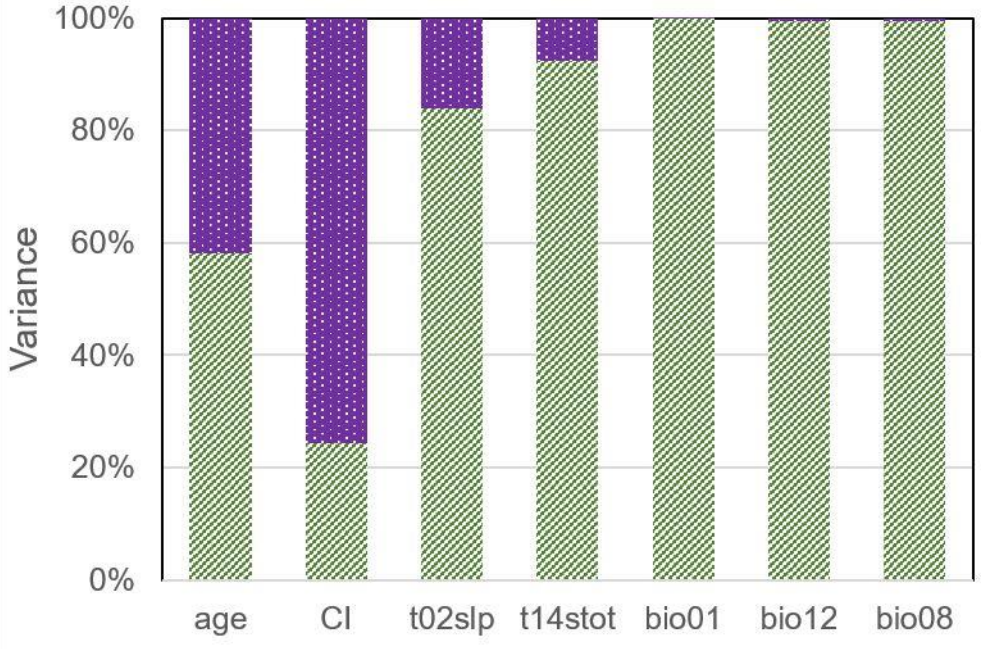

Fig. S4. **Distribution of trait variance of environmental variables**. The partitioning of variance revealed the component within populations (dotted purple bar) and among populations (striped green bars). CI: competition index assessed with the five nearest trees to the target one; t02slp: slope; t14stot: potential total solar radiation; bio01: mean annual temperature; bio12: mean annual precipitation; bio08: temperature of the wettest quarter of the year.

References

Karger DN, Conrad O, Böhner J, Kawohl T, Kreft H, Soria-Auza RW, …, Kessler M. 2017a. Climatologies at high resolution for the earth's land surface areas. *Scientific Data* 4, 170122.

Karger DN, Conrad O, Böhner J, Kawohl T, Kreft H, Soria-Auza RW, …, Kessler M. 2017b. Data from: Climatologies at high resolution for the earth's land surface areas. Dryad Digital Repository, https://doi.org/10.5061/dryad.kd1d4

Kassambara A, Mundt F. 2020. factoextra: Extract and Visualize the Results of Multivariate Data Analyses. R package version 1.0.7. https://CRAN.R-project.org/package=factoextra.

Opgenoorth, L., Dauphin, B., Benavides, R., Heer, K., Alizoti, P., Martínez-Sancho, E., … , Cavers, S. (2020). The GenTree-Platform. figshare (access link for review process https://figsharecom/s/4d57474fd63864a6dfd8)

R Core Team. 2019. R: A language and environment for statistical computing. R Foundation for Statistical Computing, Vienna, Austria. URL https://www.R-project.org/.

Appendix B. Surveyed traits: distribution, mean values and covariation

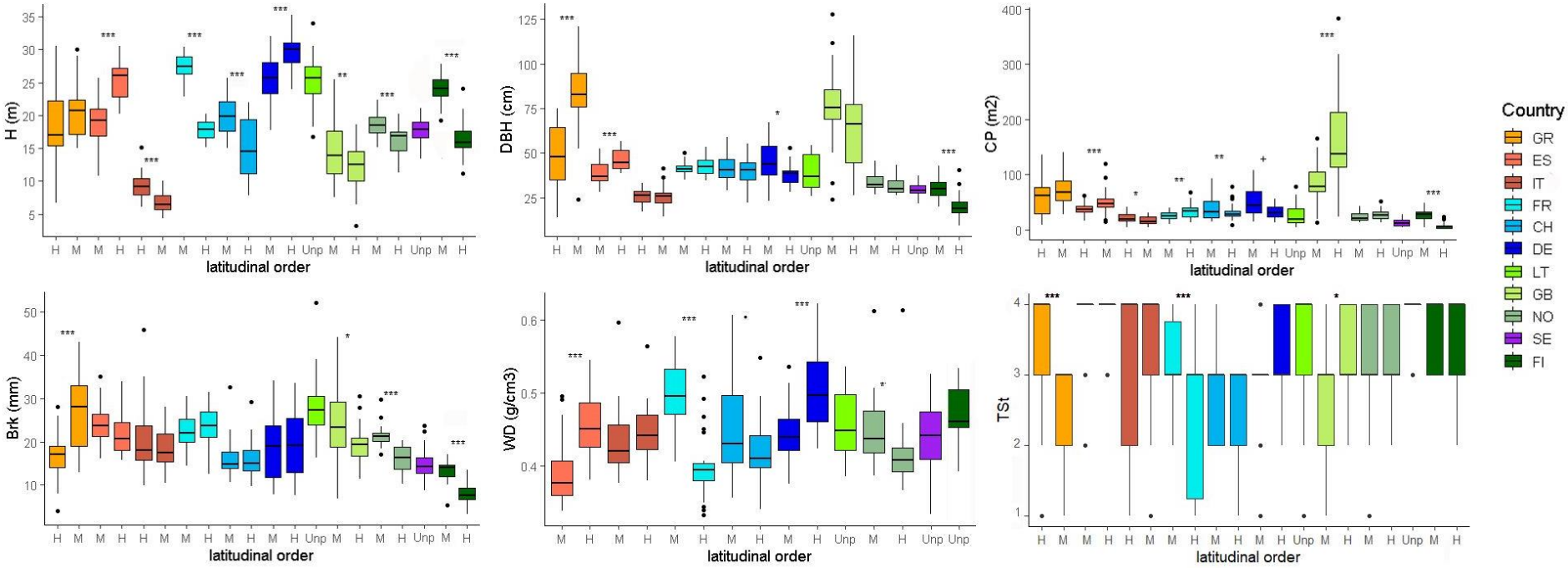

Fig. S5a. Boxplots of plant size and stem traits in each population. Populations are ordered by latitude, and sorted by the local gradient classification (M: population under milder conditions within a pair; H: population under harsher conditions within a pair; Unp: unpaired). Asterisks show significant difference between pair means (p-values: + <0.1, * <0.05, **<0.01; ***< 0.001). H: height (m), DBH: diameter at breast height (cm), CP: crown projection area (m^2), Brk: bark thickness (mm), WD: wood density (g cm^{-3}), TSt: trunk straightness. Country acronyms: ES: Spain, GR: Greece, IT: Italy, FR: France, CH: Switzerland, DE: Germany, GB: Great Britain, LT: Lithuania, NO: Norway, SE: Sweden, FI: Finland.

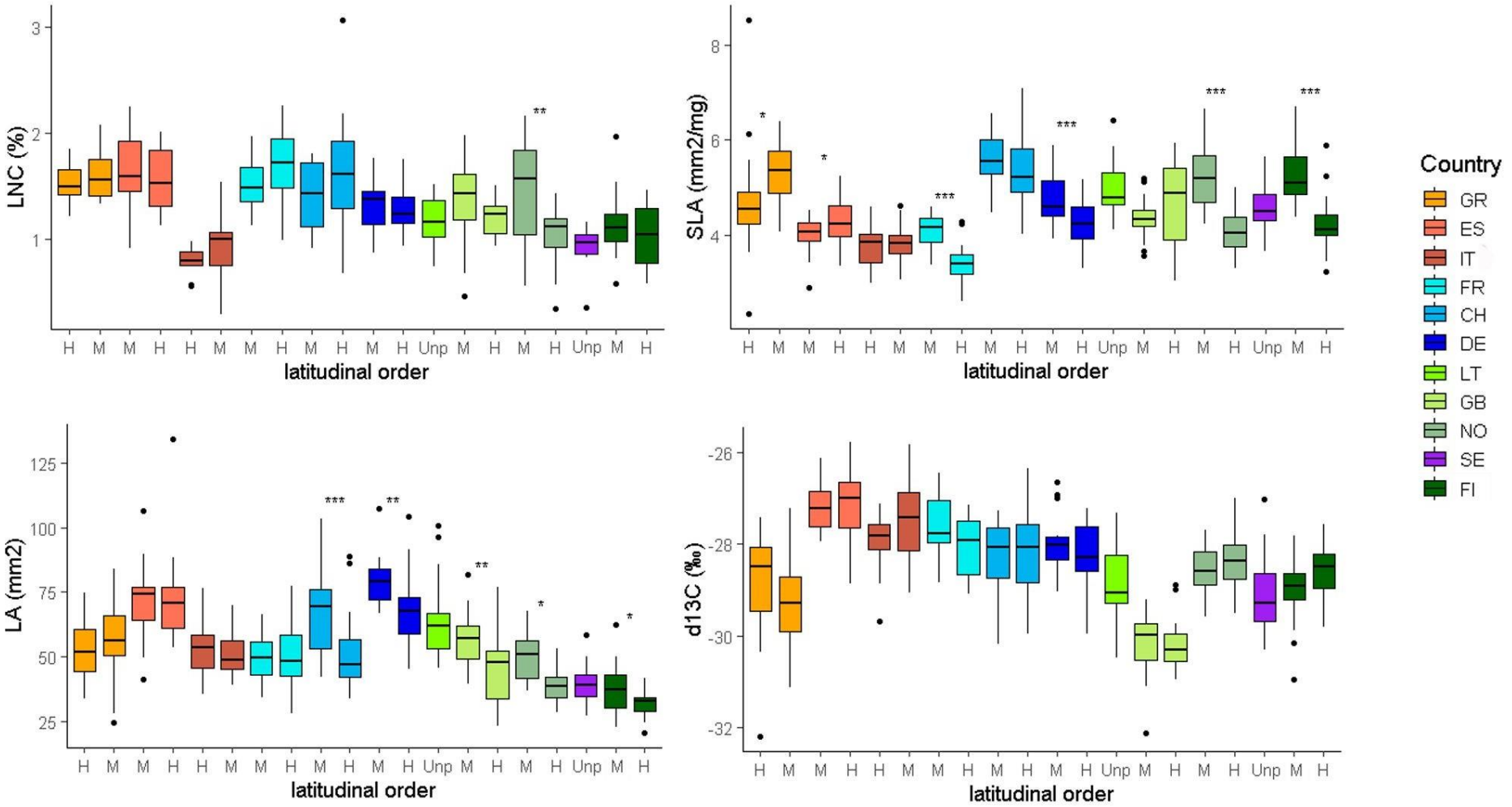

Fig. S5b. Boxplots of leaf traits in each population. Populations are ordered by latitude, and sorted by the local gradient classification (M: population under milder conditions within a pair; H: population under harsher conditions within a pair; Unp: unpaired). Asterisks show significant difference between pair means (p-values: + <0.1, * <0.05, **<0.01; ***< 0.001). LNC: leaf N content (%), SLA: specific leaf area (mm2 mg^{-1}), LA: leaf area (mm^2), d13C (‰): isotopic signature of ^{13}C. Country acronyms: ES: Spain, GR: Greece, IT: Italy, FR: France, CH: Switzerland, DE: Germany, GB: Great Britain, LT: Lithuania, NO: Norway, SE: Sweden, FI: Finland.

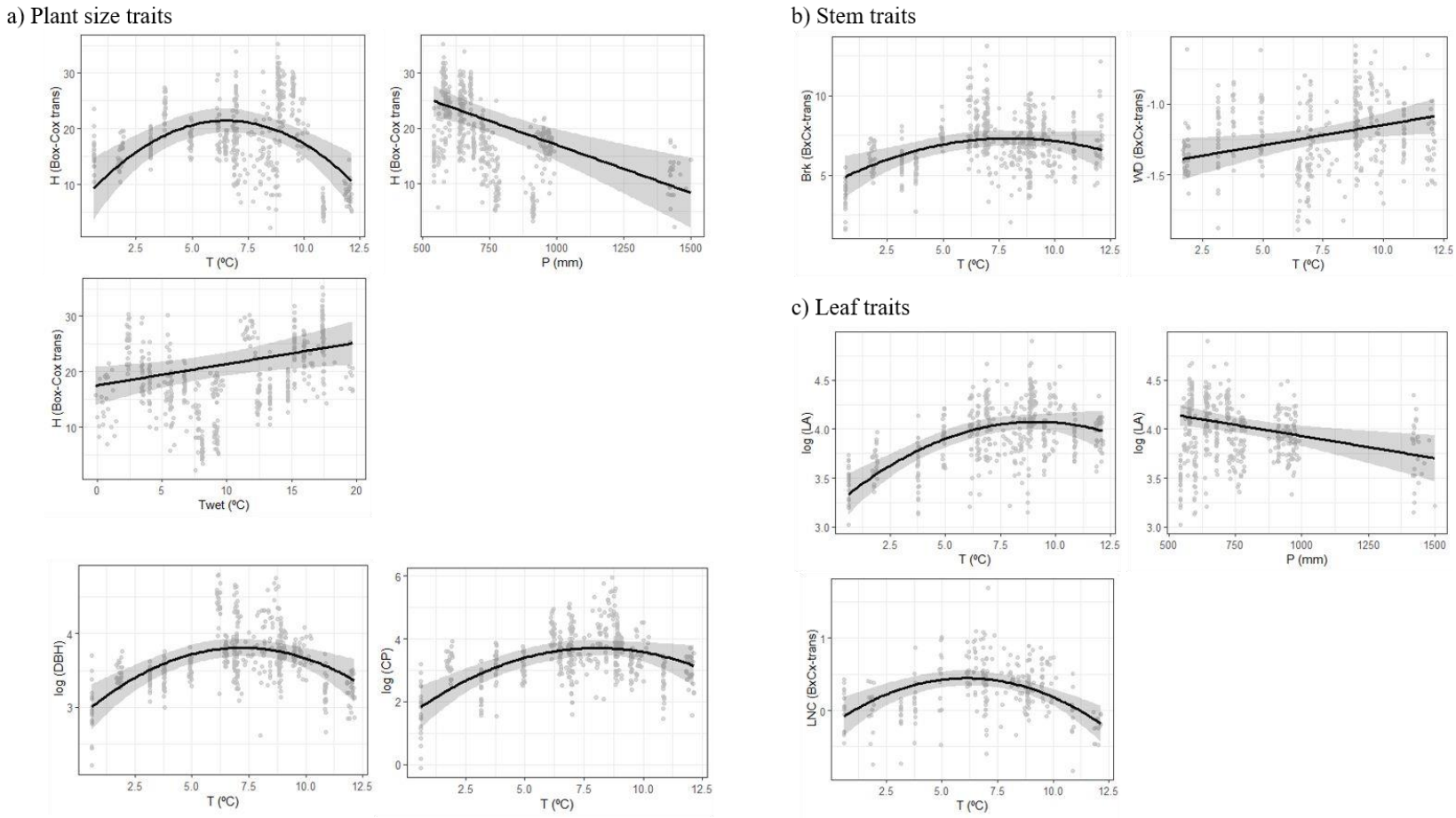

Fig. S6. Traits versus climatic variables. Plots showing linear mixed models as described in Table 2, and selected according to AIC and parsimony criteria**.** a) Traits related to plant size, b) stem traits, and c) leaf traits. Only significant effects are shown. T: mean annual temperature, P: mean annual precipitation, Twet: temperature of the wettest quarter, H: height (m), DBH: diameter at breast height (cm), CP: crown projection area (m^2), Brk: bark thickness (mm), WD: wood density (g cm^{-3}), d13C (‰): isotopic signature of ^{13}C, LNC: leaf N content (%), LA: leaf projected area (mm^2). The intervals reflect only the variance of the fixed effects, not the random effects (population), and points are the observed data.

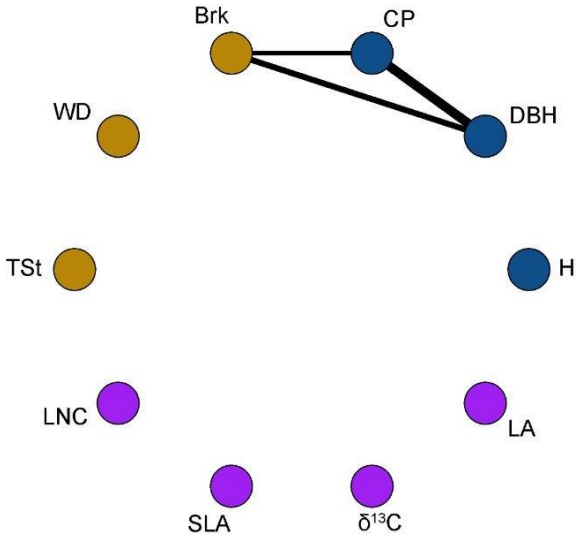

Fig. S7. **Trait correlations of *Pinus sylvestris* phenotype.** The network includes data measured in 20 populations across its European distribution. The correlations were all positive. In blue, traits related to plant size: H: height (m), DBH: diameter at breast height (cm), CP: crown projection area (m^2). In brown, stem traits: Brk: bark thickness (mm), TSt: trunk straightness, WD: wood density (g cm^{-3}). In purple, leaf traits: LNC: N content (%), SLA: specific leaf area (mm^2/mg), $\delta^{13}C$: isotopic signature of ^{13}C (‰), LA: leaf area (mm^2).

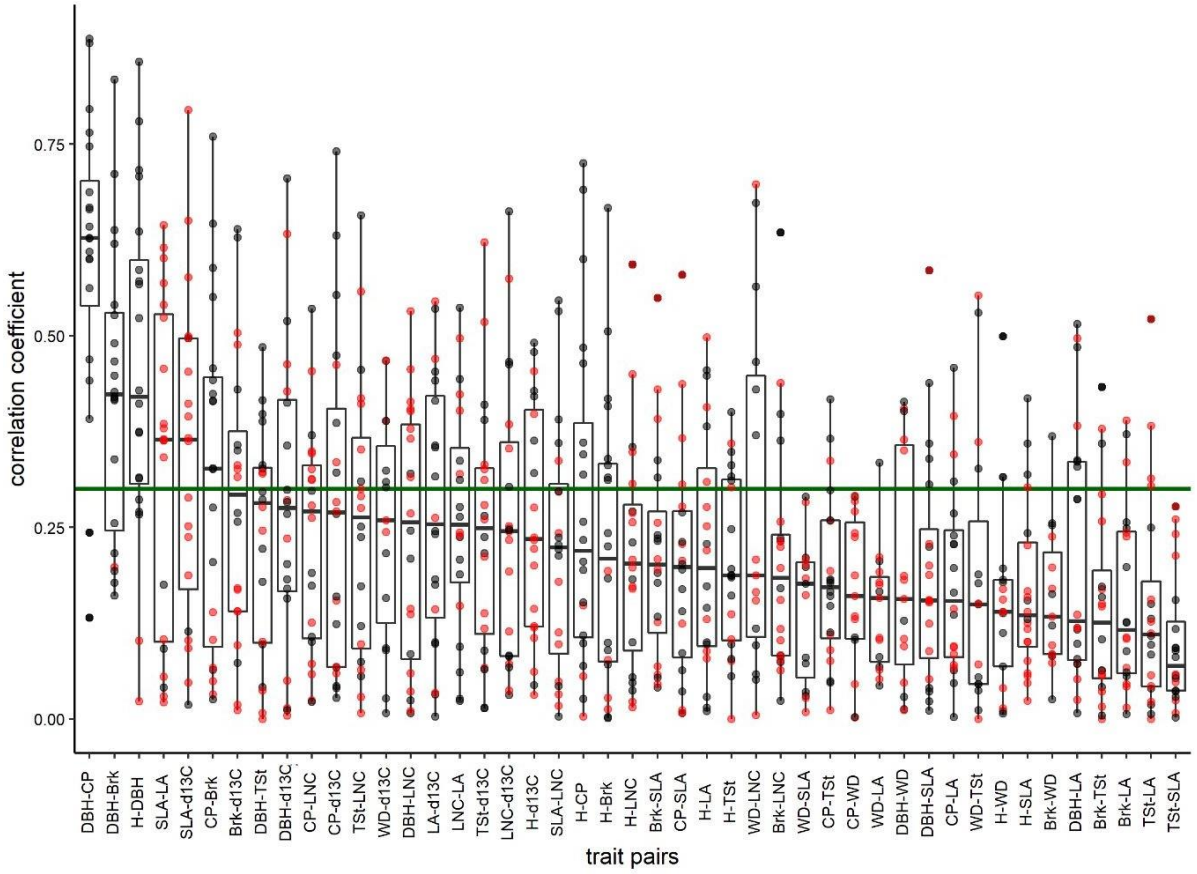

Fig. S8. Distribution of pairwise correlation coefficients. Each point represents the correlation coefficient for a given trait pair in each population. Grey represents positive correlations, red negative correlations. Green line is the threshold $|\rho| > 0.3$. Plant size and stem traits were standardised by age before the calculation of the correlation coefficients. H: tree height, DBH: diameter at breast height, CP: crown projection area, Brk: bark thickness, TSt: trunk straightness, WD: wood density, LNC: leaf N content, SLA: specific leaf area, $\delta^{13}C$: isotopic signature of ^{13}C, LA: leaf area.

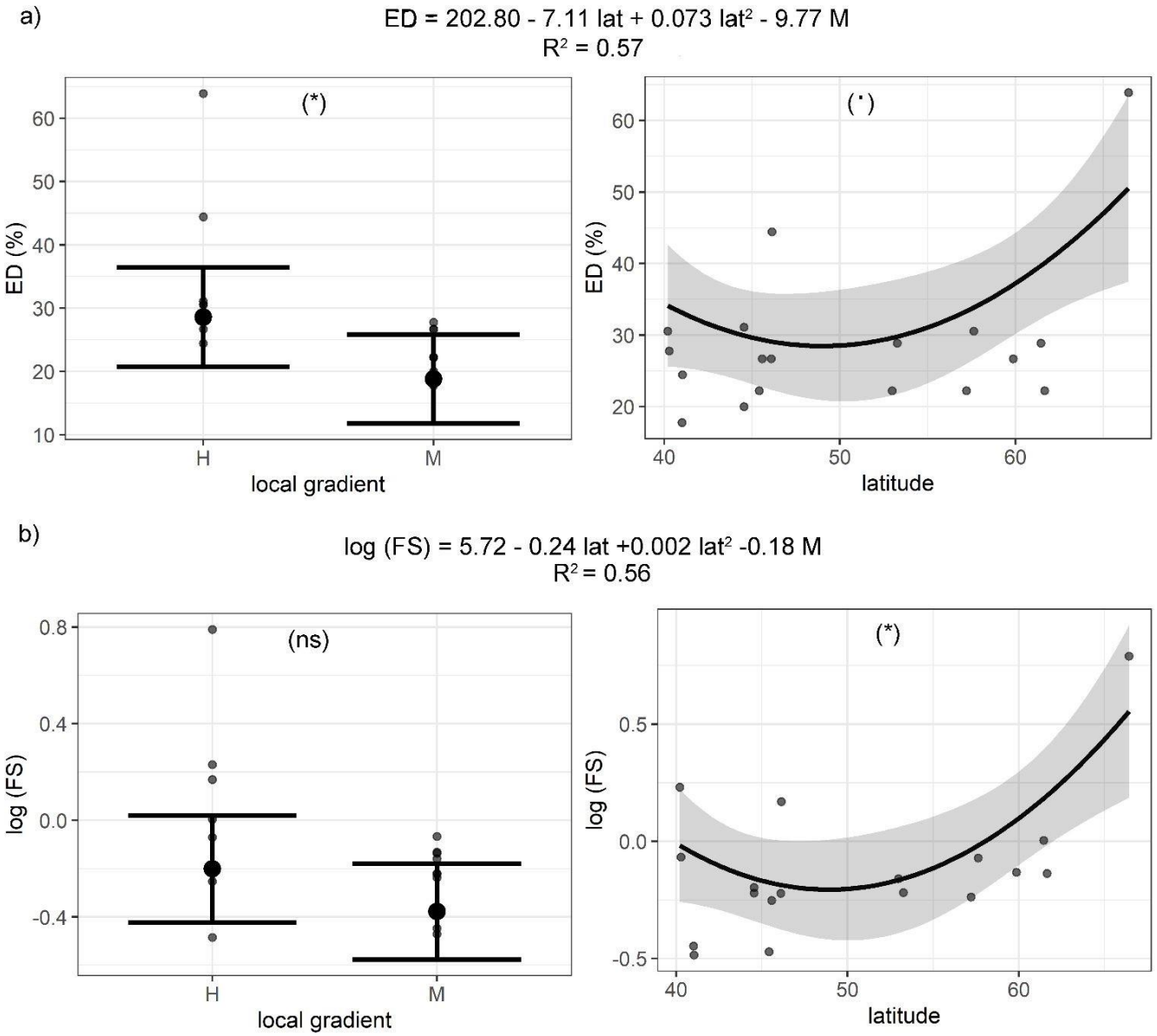

Fig. S9. Effect of local gradient and latitude on a) edge density (ED); and on b) (log) functional variability shape (FS). ED is the ratio between the number of significant correlations and all possible pairwise trait combinations, and FS is the variance of the eigenvalues of the trait correlation matrix. On the top, the expression of the optimal models and their R^2. Whiskers and grey areas represent the 95% confidence intervals. Significance level of each term shown in brackets. Points represent the observed values. M: populations under milder conditions; H: populations under harsher conditions.

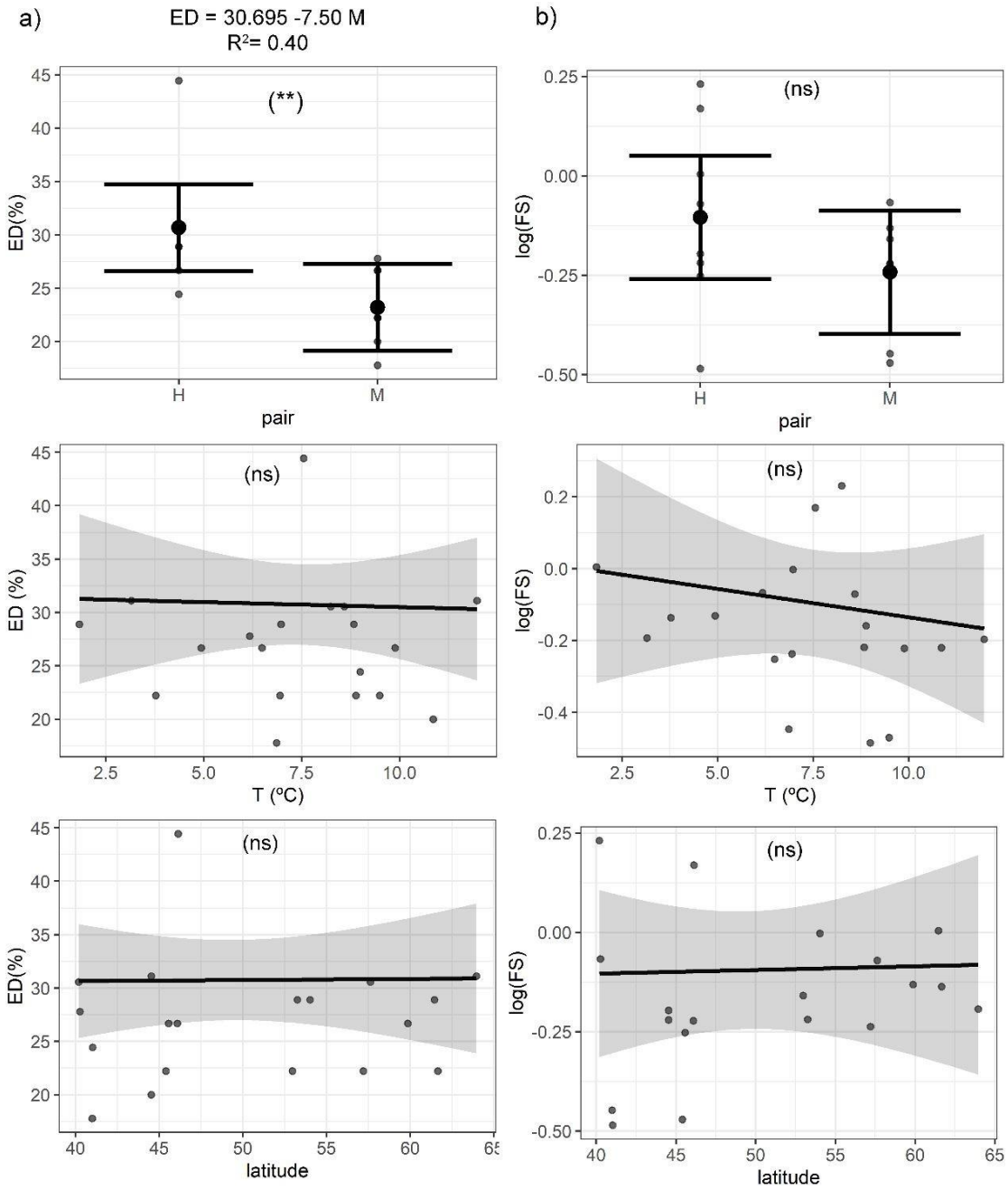

Fig S10. Effect of local gradient and climatic variables/ latitude on a) edge density (ED) and b) functional variability shape (FS) without northern-most population (FI_18). ED is the ratio between the number of significant correlations and all possible pairwise trait combinations, and FS is the variance of the eigenvalues of the trait correlation matrix. On the top, the expression of the optimal models and their R^2. For FS, none of the variables affected significantly. Whiskers and grey areas represent the 95% confidence intervals. Significance level of each term shown in brackets. Points represent the observed values. M: populations under milder conditions; H: populations under harsher conditions.

Appendix C. Model selection

Table S4. Model comparison of variables affecting trait variation for each trait. We include the ten models with lower AIC, ranked in increasing order. Models in grey are considered the best and not significantly different among them, i.e. AIC difference compared to the lowest one (ΔAIC) below 2 (Burnham & Anderson, 2002). Among the colored models, we selected the most parsimonious shown in bold and red-framed.

	df	age	CI	slp	rad	T	T2	P	Twet	AIC	ΔAIC
H	**8**	**x**				**x**	**x**	**x**	**x**	**2583.3**	**0**
	9	x	x			x	x	x	x	2583.5	-0.2
	9	x		x		x	x	x	x	2584.4	-1.1
	10	x	x	x		x	x	x	x	2584.7	-1.4
	10	x		x	x	x	x	x	x	2584.8	-1.5
	9	x			x	x	x	x	x	2584.9	-1.6
	9	x		x	x	x	x	x		2585	-1.7
	10	x	x		x	x	x	x	x	2585.1	-1.8
	11	x	x	x	x	x	x	x	x	2585.2	-1.9
	10	x	x	x	x	x	x	x		2585.5	-2.2
log (DBH)	10	x	x	x		x	x	x	x	-157.9	0
	11	x	x	x	x	x	x	x	x	-157.7	-0.2
	7	**x**	**x**			**x**	**x**			**-157.4**	**-0.5**
	8	x	x			x	x	x		-157.4	-0.5
	9	x	x			x	x	x	x	-157.4	-0.5
	8	x	x	x		x	x			-157.1	-0.8
	9	x	x	x		x	x	x		-157	-0.9
	9	x	x	x		x	x		x	-156.2	-1.7
	8	x	x			x	x		x	-156	-1.9
	10	x	x		x	x	x	x	x	-155.4	-2.5
log (CP)	**8**	**x**	**x**	**x**		**x**	**x**			**673**	**0**
	9	x	x	x	x	x	x			673.4	-0.4
	9	x	x	x		x	x		x	673.4	-0.4
	9	x	x	x		x	x	x		674.8	-1.8
	10	x	x	x	x	x	x		x	674.9	-1.9
	10	x	x	x	x	x	x	x		675.1	-2.1
	10	x	x	x		x	x	x	x	675.6	-2.6
	8	x	x		x	x	x			676.8	-3.8
	11	x	x	x	x	x	x	x	x	677	-4
	9	x	x		x	x	x	x		678.4	-5.4
bxcxBrk	**8**	**x**	**x**		**x**	**x**	**x**			**1686.7**	**0**
	9	x	x	x	x	x	x			1688.6	-1.9
	7	x	x			x	x			1688.8	-2.1
	9	x	x		x	x	x	x		1688.7	-2
	8	x	x	x		x	x			1688.9	-2.2
	9	x	x		x	x	x		x	1689.4	-2.7
	8	x	x			x	x	x		1690	-3.3
	10	x	x	x	x	x	x	x		1690.1	-3.4
	9	x	x	x		x	x	x		1690.3	-3.6
	7	x	x		x	x				1690.4	-3.7

.

	df	age	CI	slp	rad	T	T2	P	Twet	AIC	ΔAIC
bxcxWD	8	x	x	x	x	x				-66.7	-8.2
	8	x	x	x	x		x			-65.1	-9.8
	7	x		x	x	x				**-65.1**	-9.8
	9	x	x	x	x	x		x		-64.9	-10
	6	x	x						x	-64.6	-10.3
	9	x	x	x	x		x	x		-64.5	-10.4
	7	x		x	x		x			-64.4	-10.5
	8	x		x	x	x		x		-64.2	-10.7
	5	x							x	-64.2	-10.7
	7	x	x			x			x	-64.1	-10.8
TSt	**4**	**x**								**1066**	**-396.9**
	5	x					x			1066.7	-397.6
	5	x							x	1067.1	-398
	5	x						x		1067.2	-398.1
	5	x			x					1067.3	-398.2
	5	x		x						1067.8	-398.7
	6	x					x		x	1068	-398.9
	5	x	x							1068	-398.9
	5	x				x				1068.1	-399
	6	x					x	x		1068.1	-399
bxcxN	**6**				**x**	**x**	**x**			**148.3**	**-148.3**
	6					x	x		x	149.5	-149.5
	7	x			x	x	x			149.7	-149.7
	7				x	x	x		x	149.8	-149.8
	7	x				x	x		x	150.1	-150.1
	7					x	x	x	x	150.2	-150.2
	7		x		x	x	x			150.3	-150.3
	7			x	x	x	x			150.4	-150.4
	7				x	x	x	x		150.6	-150.6
	8	x			x	x	x		x	151	-151
log (SLA)	**4**		**x**							**-596.8**	**596.8**
	6		x			x	x			-595.9	595.9
	5		x	x						-595.9	595.9
	5		x				x			-595.7	595.7
	5	x	x							-595.1	595.1
	5		x			x				-595.1	595.1
	5		x					x		-594.9	594.9
	5		x						x	-594.9	594.9
	5		x		x					-594.8	594.8
	7		x	x		x	x			-594.5	594.5
log (LA)	**6**					**x**	**x**	**x**		**-74.9**	**74.90**
	7		x			x	x	x		-74.8	74.80
	7			x		x	x	x		-74.4	74.40
	8		x	x		x	x	x		-74.2	74.20
	7	x				x	x	x		-73.5	73.50
	8		x		x	x	x	x		-73.1	73.10
	8	x	x			x	x	x		-73.1	73.10
	7				x	x	x	x		-73	73.00
	8	x		x		x	x	x		-73	73.00
	7					x	x	x	x	-72.6	72.60
d13C	6	x	x		x					669.1	-669.1
	8	x	x		x		x	x		669.6	-669.6
	7	x	x		x			x		669.6	-669.6
	5		**x**		**x**					**669.7**	**-669.7**
	7	x	x		x		x			669.8	-669.8
	5	x	x							669.9	-669.9
	6	x	x				x			670	-670
	7	x	x				x	x		670.1	-670.1
	8	x	x		x	x	x			670.1	-670.1
	7	x	x		x				x	670.1	-670.1

Reference

Burnham, K.P & Anderson, D.R. 2002. Model selection and multimodel inference a practical information-theoretic approach. 2nd Edition. Springer-Verlag.